91

Two-Dimensional FIR Filters

Rashid Ansari
University of Illinois at Chicago

A. Enis Cetin
Bilkent University

91.1 Introduction

In this chapter, methods of designing two-dimensional (2-D) finite-extent impulse response (FIR) discrete-time filters are described. Two-dimensional FIR filters offer the advantages of phase linearity and guaranteed stability, which makes them attractive in applications. Over the years an extensive array of techniques for designing 2-D FIR filters has been accumulated [14, 30, 23]. These techniques can be conveniently classified into the two categories of general and specialized designs. Techniques in the category of general design are intended for approximation of *arbitrary* desired frequency responses usually with no structural constraints on the filter. These techniques include approaches such as windowing of the ideal impulse response [22] or the use of suitable optimality criteria possibly implemented with iterative algorithms. On the other hand, techniques in the category of special design are applicable to restricted classes of filters, either due to the nature of the response being approximated or due to imposition of structural constraints on the filter used in the design. The specialized designs are a consequence of the observation that commonly used filters have characteristic underlying features that can be exploited to simplify the problem of design and implementation. The stopbands and passbands of filters encountered in practice are often defined by straight line, circular or elliptical boundaries. Specialized design methodologies have been developed for handling these cases and they are typically based on techniques such as the transformation of one-dimensional (1-D) filters or the rotation and translation of separable filter responses. If the desired response possesses symmetries, then the symmetries imply relationships among the filter coefficients which are exploited in both the design and the implementation of the filters. In some design problems it may be advantageous to impose structural constraints in the form of parallel and cascade connections.

The material in this chapter is organized as follows. A preliminary discussion of characteristics of 2-D FIR filters and issues relevant to the design methods appears in Section 91.2. Following this, methods of general and special FIR filter design are described in Sections 91.3 and 91.4, respectively. Several examples of design illustrating the procedure are also presented. Issues in 2-D FIR filter implementation are briefly discussed in Section 91.5. Finally, additional topics are outlined in Section 91.6, and a list of sources for further information is provided.

91.2 Preliminary Design Considerations

In any 2-D filter design there is a choice between FIR and IIR filters, and their relative merits are briefly examined next. Two-dimensional FIR filters offer certain advantages over 2-D IIR filters as a result of which FIR filters have found widespread use in applications such as image and video processing. One key attribute of an FIR filter is that it can be designed with strictly linear passband phase, and it can be implemented with small delays without the need to reverse the signal array during processing. A 2-D FIR filter impulse response has only a finite number of nonzero samples which guarantees stability. On the other hand, stability is difficult to test in the case of 2-D IIR filters due to the absence of a 2-D counterpart of the fundamental theorem of algebra, and a 2-D polynomial is almost never factorizable. If a 2-D FIR filter is implemented nonrecursively with finite precision, then it does not exhibit limit cycle oscillations. Arithmetic quantization noise and coefficient quantization effects in FIR filter implementation are usually very low. A key disadvantage of FIR filters is that they typically have higher computational complexity than IIR filters for meeting the same specifications, especially in cases where the specifications are stringent.

The term 2-D FIR filter refers to a linear shift-invariant system whose input–output relation is represented by a convolution [14]

$$y(n_1,n_2)=\sum_{(k_1,k_2)\in}\sum_{I}h(k_1,k_2)x(n_1-k_1,n_2-k_2), \tag{91.1}$$

where $x(n_1, n_2)$ and $y(n_1, n_2)$ are the input and the output sequences, respectively, $h(n_1, n_2)$ is the impulse response sequence, and I is the support of the impulse response sequence. FIR filters have compact support, meaning that only a finite number of coefficients are nonzero. This makes the impulse response sequence of FIR filters absolutely summable, thereby ensuring filter stability. Usually the filter support, I, is chosen to be a rectangular region centered at the origin, e.g., $I = \{(n_1,n_2):-N_1 \le n_1 \le N_1,-N_2 \le n_2 \le N_2\}$. However, there are some important cases where it is more advantageous to select a non-rectangular region as the filter support [32].

Once the extent of the impulse response support is determined, the sequence $h(n_1, n_2)$ should be chosen in order to meet given filter specifications under suitable approximation criteria. These aspects are elaborated on in the next subsection. This is followed by a discussion of phase linearity and filter response symmetry considerations and then some guidelines on using the design methods are provided.

Filter Specifications and Approximation Criteria

The problem of designing a 2-D FIR filter consists of determining the impulse response sequence, $h(n_1, n_2)$, or its system function, $H(z_1, z_2)$, in order to satisfy given requirements on the filter response. The filter requirements are usually specified in the frequency domain, and only this case is considered here. The frequency response,[1] $H(\omega_1, \omega_2)$, corresponding to the impulse response $h(n_1, n_2)$, with a support, I, is expressed as

$$H(\omega_1,\omega_2)=\sum_{(n_1,n_2)}\sum_{\in I}h(n_1,n_2)e^{-j(\omega_1 n_1+\omega_2 n_2)}. \tag{91.2}$$

[1]Here $\omega_1 = 2\pi f_1$ and $\omega_2 = 2\pi f_2$ are the horizontal and vertical angular frequencies, respectively.

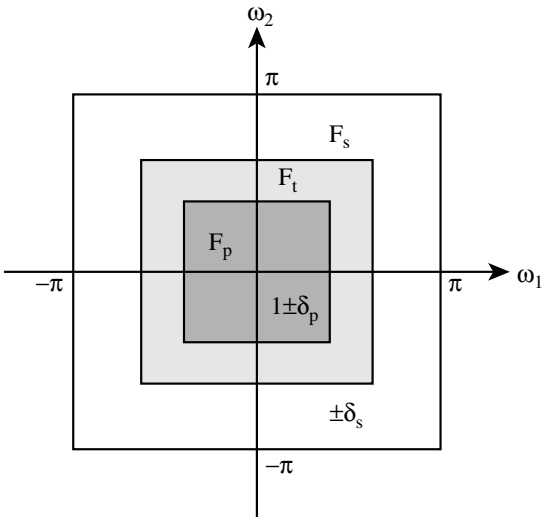

FIGURE 91.1 Frequency response specifications for a 2-D lowpass filter ($|H(\omega_1, \omega_2) - 1| \leq \delta_p$ for $(\omega_1, \omega_2) \in F_p$ and $|H(\omega_1, \omega_2)| \leq \delta_s$ for $(\omega_1, \omega_2) \in F_s$).

Note that $H(\omega_1, \omega_2) = H(\omega_1 + 2\pi, \omega_2) = H(\omega_1, \omega_2 + 2\pi)$ for all (ω_1, ω_2). In other words, $H(\omega_1, \omega_2)$ is a periodic function with a period 2π in both ω_1 and ω_2. This implies that by defining $H(\omega_1, \omega_2)$ in the region $\{-\pi < \omega_1 \leq \pi, -\pi < \omega_2 \leq \pi\}$, the frequency response of the filter for all (ω_1, ω_2) is determined.

For 2-D FIR filters the specifications are usually given in terms of the magnitude response, $|H(\omega_1, \omega_2)|$. Attention in this chapter is confined to the case of a two-level magnitude design, where the desired magnitude levels are either 1.0 (in the passband) or 0.0 (in the stopband). Some of the procedures can be easily modified to accommodate multilevel magnitude specifications, as, for instance, in a case that requires the magnitude to increase linearly with distance from the origin in the frequency domain.

Consider the design of a 2-D FIR lowpass filter whose specifications are shown in Fig. 91.1. The magnitude of the lowpass filter ideally takes the value 1.0 in the passband region, F_p, which is centered around the origin, $(\omega_1, \omega_2) = (0, 0)$, and 0.0 in the stopband region, F_s. As a magnitude discontinuity is not possible with a finite filter support, I, it is necessary to interpose a transition region, F_t, between F_p and F_s. Also, magnitude bounds $|H(\omega_1, \omega_2) - 1| \leq \delta_p$ in the passband and $|H(\omega_1, \omega_2)| \leq \delta_s$ in the stopband are specified, where the parameters δ_p and δ_s are positive real numbers, typically much less than 1.0. The frequency response $H(\omega_1, \omega_2)$ is assumed to be real. Consequently, the lowpass filter is specified in the frequency domain by the regions, F_p, F_s, and the tolerance parameters, δ_p and δ_s. A variety of stopband and passband shapes can be specified in a similar manner.

In order to meet given specifications, an adequate filter order (the number of non-zero impulse response samples) needs to be determined. If the specifications are stringent, with tight tolerance parameters and small transition regions, then the filter support region, I, must be large. In other words, there is a trade-off between the filter support region, I, and the frequency domain specifications. In the general case the filter order is not known *a priori*, and may be determined either through an iterative process or using estimation rules if available. If the filter order is given, then in order to determine an optimum solution to the design problem, an appropriate optimality criterion is needed. Commonly used criteria in 2-D filter design are minimization of the L_p norm, p finite, of the approximation error, or the L_∞ norm. If desired, a maximal flatness requirement at desired frequencies can be imposed [24]. It should be noted that if the specifications are given in terms of the tolerance bounds on magnitude, as described above, then the use of L_∞ criterion is appropriate. However, the use of other criteria such as a weighted L_2 norm can serve to arrive at an almost minimax solution [2].

Zero-Phase FIR Filters and Symmetry Considerations

Phase linearity is important in many filtering applications. As in the 1-D case, a number of conditions for phase linearity can be obtained depending on the nature of symmetry. But the discussion here is limited to the case of "zero phase" design, with a purely real frequency response. A salient feature of 2-D FIR filters is that realizable FIR filters, which have purely real frequency responses, are easily designed.

The term "zero phase" is somewhat misleading in the sense that the frequency response may be negative at some frequencies. The term should be understood in the sense of "zero phase in passband" because the passband frequency response is within a small deviation of the value 1.0. The frequency response may assume negative values in the stopband region where phase linearity is immaterial. In frequency domain, the zero-phase or real frequency response condition corresponds to

$$H(\omega_1,\omega_2) = H^*(\omega_1,\omega_2), \tag{91.3}$$

where $H^*(\omega_1,\omega_2)$ denotes the complex conjugate of $H(\omega_1,\omega_2)$. The condition (91.3) is equivalent to

$$h(n_1,n_2) = h^*(-n_1,-n_2) \tag{91.4}$$

in the spatial-domain. Making a common practical assumption that $h(n_1, n_2)$ is real, the above condition reduces to

$$h(n_1,n_2) = h(-n_1,-n_2), \tag{91.5}$$

implying a region of support with the above symmetry about the origin.

Henceforth, only the design of zero-phase FIR filters is considered. With $h(n_1, n_2)$ real, and satisfying (91.5), the frequency response, $H(\omega_1, \omega_2)$, is expressed as

$$\begin{aligned} H(\omega_1,\omega_2) &= h(0,0) + \sum_{(n_1,n_2)\in I_1} h(n_1,n_2)e^{-j(\omega_1 n_1+\omega_2 n_2)} + \sum_{(n_1,n_2)\in I_2} h(n_1,n_2)e^{-j(\omega_1 n_1+\omega_2 n_2)} \\ &= h(0,0) + \sum_{(n_1,n_2)\in I_1} 2h(n_1,n_2)\cos(\omega_1 n_1 + \omega_2 n_2), \end{aligned} \tag{91.6}$$

where I_1 and I_2 are disjoint regions such that $I_1 \cup I_2 \cup \{(0,0)\} = I$, and if $(n_1,n_2)\in I_1$, then $(-n_1,-n_2)\in I_2$.

In order to understand the importance of phase linearity in image processing, consider an example that illustrates the effect of nonlinear-phase filters on images. In Fig. 91.2(a), an image that is corrupted by white Gaussian noise is shown. This image is filtered with a nonlinear-phase low-pass filter and the resultant image is shown in Fig. 91.2(b). It is observed that edges and textured regions are severely distorted in Fig. 91.2(b). This is due to the fact that the spatial alignment of frequency components that define an edge in the original is altered by the phase non-linearity. The same image is also filtered with a zero-phase lowpass filter, $H(\omega_1,\omega_2)$, which has the same magnitude characteristics as the nonlinear-phase filter. The resulting image is shown in Fig. 91.2(c). It is seen that the edges are perceptually preserved in Fig. 91.2(c), although blurred due to the lowpass nature of the filter. In this example, a separable zero-phase lowpass filter, $H(\omega_1,\omega_2) = H_1(\omega_1)\,H_1(\omega_2)$, is used, where $H_1(\omega)$ is a 1-D Lagrange filter with a cut-off $\pi/2$. In spatial domain $h(n_1, n_2) = h_1(n_1)\ h_1(n_2)$ where $h_1(n) = \{\ldots, 0, -1/32, 0, 9/32, 1/2, 9/32, 0, -1/32, 0, \ldots,\}$ is the impulse response of the 7th order symmetric (zero-phase) 1-D Lagrange filter. The nonlinear-phase filter is a cascade of the above zero-phase filter with an allpass filter.

In some filter design problems, symmetries in frequency domain specifications can be exploited by imposing restrictions on the filter coefficients and the shape of the support region for the impulse response. A variety of symmetries that can be exploited is extensively studied in [32, 44, 45]. For example, a condition often encountered in practice is the symmetry with respect to each of the two frequency axes. In this case, the frequency response of a zero-phase filter satisfies

$$H(\omega_1,\omega_2) = H(-\omega_1,\omega_2) = H(\omega_1,-\omega_2). \tag{91.7}$$

This yields an impulse response that is symmetric with respect to the n_1 and n_2 axes, i.e.,

$$h(n_1,n_2) = h(-n_1,n_2) = h(n_1,-n_2). \tag{91.8}$$

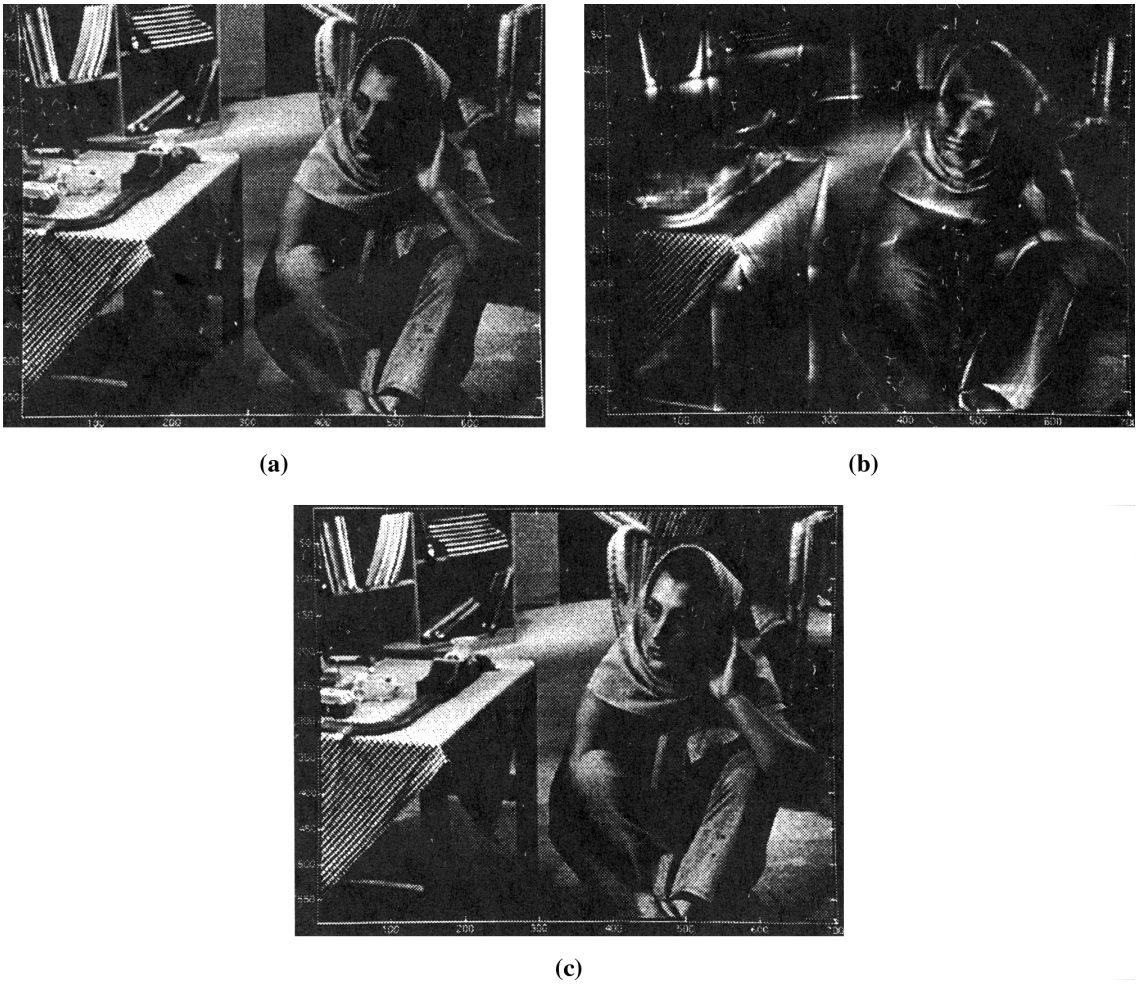

FIGURE 91.2 (a) Original image of 696 × 576 pixels; (b) nonlinear phase lowpass filtered image; (c) zero-phase lowpass filtered image.

By imposing symmetry conditions, one reduces the number of independently varying filter coefficients that must be determined in the design. This can be exploited in reducing both the computational complexity of the filter design and the number of arithmetic operations required in the implementation.

Guidelines On the Use of the Design Techniques

The design techniques described in this chapter are classified into the two categories of general and specialized designs. The user should use the techniques of general design in cases requiring approximation of arbitrary desired frequency responses, usually with no structural constraints on the filter. The specialized designs are recommended in cases where filters exhibit certain underlying features that can be exploited to simplify the problem of design and implementation.

In the category of general design, four methods are described. Of these, the windowing procedure is quick and simple. It is useful in situations where implementation efficiency is not critical, especially in single-use applications. The second procedure is based on linear programming, and is suitable for design problems where equiripple solutions are desired to meet frequency domain specifications. The remaining two procedures may also be used for meeting frequency domain specifications, and lead to nearly equiripple solution. The third procedure provides solutions for L_p approximations. The fourth procedure is an iterative procedure that is easy to implement, and is convenient in situations where additional constraints are to be placed on the filter.

In the category of specialized design described here, the solutions are derived from 1-D filters. These often lead to computationally efficient implementation, and are recommended in situations where low

implementation complexity is critical, and the filter characteristics possess features that can be exploited in the design. An important practical class of filters is one where specifications can be decomposed into a set of separable filter designs requiring essentially the design of suitable 1-D filters. Here the separable design procedure should be used. Another class of filters is one where the passbands and stopbands are characterized by circular, elliptical, or special straight-line boundaries. In this case a frequency transformation method, called the McClellan transformation procedure, is convenient to use. The desired 2-D filter constant-magnitude contours are defined by a proper choice of parameters in a transformation of variables applied to a 1-D zero-phase filter. Finally, in some cases filter specifications are characterized by ideal frequency responses in which passbands and stopbands are separated by straight-line boundaries that are not suitable for applying the McClellan transformation procedure. In this case the design may be carried out by nonrectangular transformations and sampling grid conversions. The importance of this design method stems from the implementation efficiency that results from a generalized notion of separable processing.

91.3 General Design Methods for Arbitrary Specifications

Some general methods of meeting arbitrary specifications are now described. These are typically based on extending techniques of 1-D design. However, there are important differences. The Parks-McClellan procedure for minimax approximation based on the alternation theorem does not find a direct extension. This is because the set of cosine functions used in the 2-D approximation does not satisfy the Haar condition on the domain of interest [25], and the Chebyshev approximation does not have a unique solution. However, techniques that employ exchange algorithms have been developed for the 2-D case [25, 36, 20].

Here we consider four procedures in some detail. The first technique is based on windowing. It is a simple, but is not optimum for Chebyshev approximation. The second technique is based on frequency sampling, and this can be used to arrive at equiripple solutions using linear programming. Finally, two techniques for arriving iteratively at a nearly equiripple solution are described. The first of these is based on L_p approximations using nonlinear optimization. The second is based on the use of alternating projections in the sample and the frequency domains.

Design of 2-D FIR Filters by Windowing

This design method is basically an extension of the window-based 1-D FIR filter design to the case of 2-D filters. An ideal impulse response sequence, which is usually an infinite-extent sequence, is suitably windowed to make the support finite. One-dimensional FIR filter design by windowing and classes of 1-D windows are described in detail in Section 91.2.

Let $h_{id}(n_1, n_2)$ and $H_{id}(\omega_1,\omega_2)$ be the impulse and frequency responses of the ideal filter, respectively. The impulse response of the required 2-D filter, $h(n_1, n_2)$, is obtained as a product of the ideal impulse response sequence and a suitable 2-D window sequence which has a finite extent support, I, that is,

$$h(n_1,n_2)=\begin{cases} h_{id}(n_1,n_2)w(n_1,n_2) & (n_1,n_2)\in I, \\ 0, & \text{otherwise} \end{cases} \tag{91.9}$$

where $w(n_1, n_2)$ is the window sequence. The resultant frequency response, $H(\omega_1,\omega_2)$, is a smoothed version of the ideal frequency response as $H(\omega_1,\omega_2)$ is related to the $H_{id}(\omega_1,\omega_2)$ via the periodic convolution, that is,

$$H(\omega_1,\omega_2)=\frac{1}{4\pi^2}\int_{-\pi}^{\pi}\int_{-\pi}^{\pi}H_{id}(\Omega_1,\Omega_2)W(\omega_1-\Omega_1,\omega_2-\Omega_2)d\Omega_1 d\Omega_2, \tag{91.10}$$

where $W(\omega_1,\omega_2)$ is the frequency response of the window sequence, $w(n_1, n_2)$.

As in the 1-D case, a 2-D window sequence, $w(n_1, n_2)$, should satisfy three requirements:

1. It must have a finite-extent support, I.
2. Its discrete-space Fourier transform should in some sense approximate the 2-D impulse function, $\delta(\omega_1,\omega_2)$.
3. It should be real, with a zero-phase discrete-space Fourier transform.

Usually 2-D windows are derived from 1-D windows. Three methods of constructing windows are briefly examined. One method is to obtain a separable window from two 1-D windows, that is,

$$w_r(n_1,n_2) = w_1(n_1)w_2(n_2), \tag{91.11}$$

where $w_1(n)$ and $w_2(n)$ are the 1-D windows. Thus, the support of the resultant 2-D window, $w_r(n_1, n_2)$, is a rectangular region. The frequency response of the 2-D window is also separable, i.e., $W_r(\omega_1,\omega_2) = W_1(\omega_1)\, W_2(\omega_2)$.

The second method of constructing a window, due to Huang [22], consists of sampling the surface generated by rotating a 1-D continuous-time window, $w(t)$, as follows:

$$w_c(n_1,n_2) = w\left(\sqrt{n_1^2 + n_2^2}\right), \tag{91.12}$$

where $w(t) = 0$, $t \geq N$. The impulse response support is $I = \{n_1, n_2: \sqrt{n_1^2 + n_2^2} < N\}$. Note that the 2-D Fourier transform of the $w_c(n_1, n_2)$ is not equal to the circularly rotated version of the Fourier transform of $w(t)$.

Finally, in the third method, proposed by Yu and Mitra [53], the window is constructed by using a 1-D to 2-D transformation belonging to a class called the McClellan transformations [33]. These transformations are discussed in greater detail in Section 91.4. Here we consider a special case of the transform that produces approximately circular contours in the 2-D frequency domain. Briefly, the discrete-space frequency transform of the 2-D window sequence obtained with a McClellan transformation applied to a 1-D window is given by

$$\begin{aligned} T(\omega_1,\omega_2) &= \sum_{n=-N}^{N} w(n)e^{-j\omega n}\Big|_{\cos(\omega)=0.5\cos(\omega_1)+0.5\cos(\omega_2)+0.5\cos(\omega_1)\cos(\omega_2)-0.5} \\ &= w(0) + \sum_{n=1}^{N} w(n)\cos(n\omega)\Big|_{\cos(\omega)=0.5\cos(\omega_1)+0.5\cos(\omega_2)+0.5\cos(\omega_1)\cos(\omega_2)-0.5} \\ &= \sum_{n=0}^{N} b(n)\cos^n(\omega)\Big|_{\cos(\omega)=0.5\cos(\omega_1)+0.5\cos(\omega_2)+0.5\cos(\omega_1)\cos(\omega_2)-0.5} \end{aligned} \tag{91.13}$$

where $w(n)$ is an arbitrary symmetric 1-D window of duration $2N + 1$ centered at the origin, and the coefficients, $b(n)$, are obtained from $w(n)$ via Chebyshev polynomials [33]. After some algebraic manipulations it can be shown that

$$T(\omega_1,\omega_2) = \sum_{n_1=-N}^{N}\sum_{n_2=-N}^{N} w_t(n_1,n_2)e^{-j(n_1\omega_1+n_2\omega_2)}, \tag{91.14}$$

where $w_t(n_1, n_2)$ is a zero-phase 2-D window of size $(2N+1)\times(2N+1)$ obtained by using the McClellan transformation.

The construction of 2-D windows using the above three methods is now examined. In the case of windows obtained by the separable and the McClellan transformation approaches, the 1-D prototype is a Hamming window,

$$w_h(n) = \begin{cases} 0.54 + 0.46\cos(\pi n/N), & |n| < N, \\ 0, & \text{otherwise.} \end{cases} \tag{91.15}$$

In the second case $w_c(n_1, n_2) = 0.54 + 0.46\cos(\pi\sqrt{n_1^2 + n_2^2}/N)$. By selecting $w_1(n) = w_2(n) = w_h(n)$ in (91.11) we get a 2-D window, $w_r(n_1, n_2)$, of support $I = \{|n_1| < N, |n_2| < N\}$ which is a square-shaped symmetric region centered at the origin. For $N = 6$ the region of support, I contains $11 \times 11 = 121$ points. Figure 91.3(a) shows the frequency response of this window. A second window is designed by using (91.12), i.e., $w_c(n_1, n_2) = w_h(\sqrt{n_1^2 + n_2^2})$. For $N = 6$ the frequency response of this filter is shown in Fig. 91.3(b). The region of support is almost circular and it contains 113 points. From these examples, it is seen that the 2-D windows may not behave as well as 1-D windows. Speake and Mersereau [46] compared these two methods and observed that the main-lobe width and the highest attenuation level of the side-lobes of the 2-D windows differ from their 1-D prototypes.

Let us construct a 2-D window by the McClellan transformation with a 1-D Hamming window of order 13 ($N = 6$) as the prototype. The frequency response of the 2-D window, $w_t(n_1, n_2)$, is shown in Fig. 91.3(c). The frequency response of this window is almost circularly symmetric and it preserves the features of its 1-D prototype.

Consider the design of a circularly symmetric low-pass filter. The ideal frequency response for $(\omega_1, \omega_2) \in [-\pi, \pi] \times [-\pi, \pi]$ is given by

$$H_{id}(\omega_1, \omega_2) = \begin{cases} 1, & \sqrt{\omega_1^2 + \omega_2^2} \le \omega_c, \\ 0, & \text{otherwise.} \end{cases} \tag{91.16}$$

whose impulse response is given by

$$h_{id}(n_1, n_2) = \frac{\omega_c J_1\left(\omega_c\sqrt{n_1^2 + n_2^2}\right)}{2\pi\sqrt{n_1^2 + n_2^2}}, \tag{91.17}$$

where $J_1(.)$ is the first-order Bessel function of the first kind, and ω_c is the cutoff frequency. The frequency response of the 2-D FIR filter obtained with a rectangular window of size $2 \times 5 + 1$ by $2 \times 5 + 1$ is shown in Fig. 91.4(a). Note the Gibbs-phenomenon type ripples at the passband edges. In Fig. 91.4(b) the separable window of Fig. 91.3(a), derived from a Hamming window, is used to design the 2-D filter. Note that this 2-D filter has smaller ripples at the passband edges.

In windowing methods, it is often assumed that $H_{id}(\omega_1, \omega_2)$ is given. However, if the specifications are given as described in Section 91.2, then a proper $H_{id}(\omega_1, \omega_2)$ should be constructed. The ideal magnitudes are either 1.0 (in passband) or 0.0 (in stopband). However, there is a need to define a *cutoff* boundary, which lies within the transition band. This can be accomplished by using a suitable notion of "midway" cutoff between the transition boundaries. In practical cases where transition boundaries are given in terms of straight-line segments or smooth curves such as circles and ellipses, the construction of "midway" cutoff boundary is relatively straightforward. The ideal impulse response, $h_{id}(n_1, n_2)$, is computed from the desired frequency response, $H_{id}(\omega_1, \omega_2)$, either analytically (if possible), or by using the discrete Fourier transform (DFT). In the latter case the desired response, $H_{id}(\omega_1, \omega_2)$, is first sampled on a rectangular grid in the Fourier domain, then an inverse DFT computation is carried out via a 2-D fast Fourier transform (FFT) algorithm to obtain an approximation to the sequence $h_{id}(n_1, n_2)$. The resulting sequence is an aliased version of the ideal impulse response. Therefore, a sufficiently dense grid should be used in order to reduce the effects of aliasing.

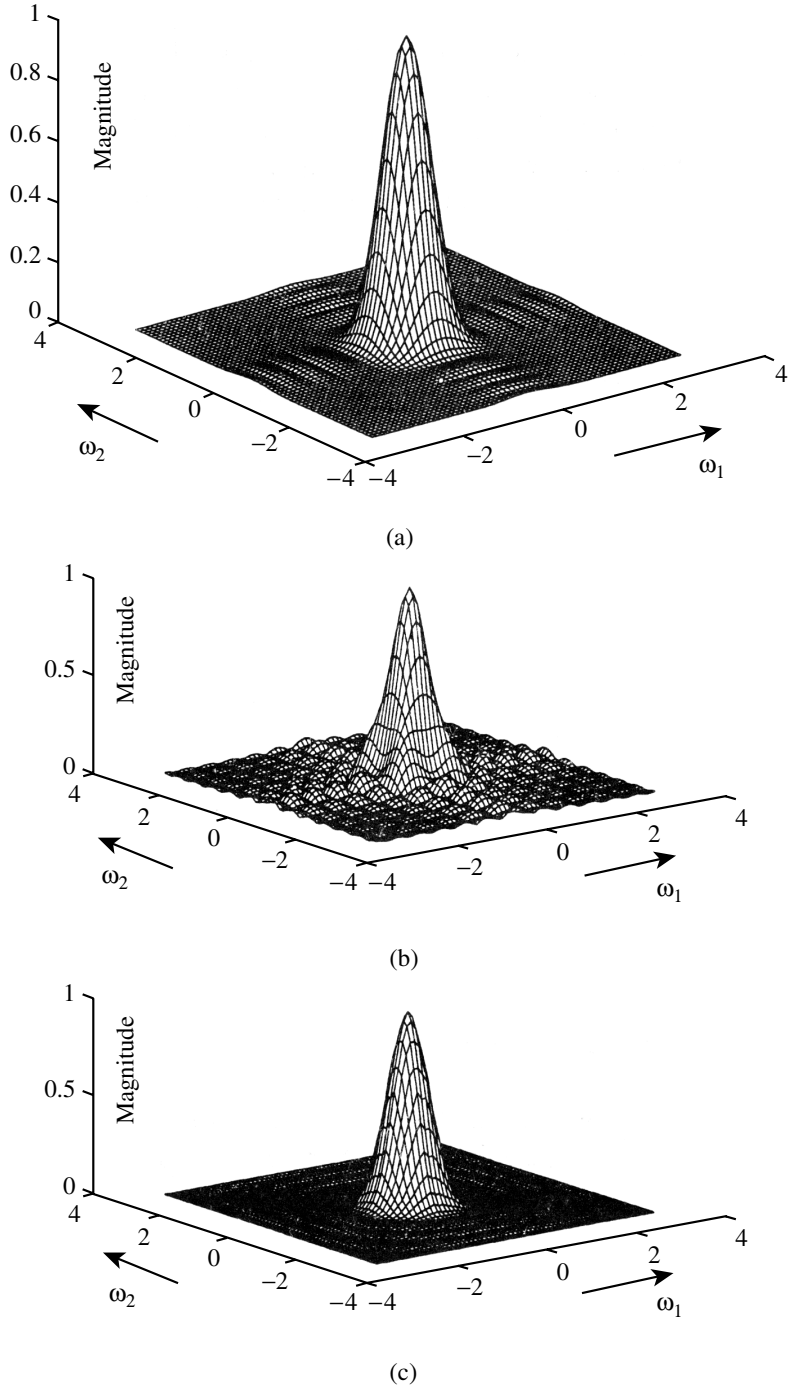

FIGURE 91.3 Frequency responses of the (a) separable, (b) Huang, and (c) McClellan 2-D windows generated from a Hamming window of order 13 ($N = 6$).

In practice, several trials may be needed to design the final filter satisfying bounds both in the passbands and stopbands. The filter support is adjusted to obtain the smallest order to meet given requirements.

Filter design with windowing is a simple approach that is suitable for applications where a quick and non-optimal design is needed. Additional information on windowing can be found in [26, 46].

Frequency Sampling and Linear Programming Based Method

This method is based on the application of the sampling theorem in the frequency domain. Consider the design of a 2-D filter with impulse response support of $N_1 \times N_2$ samples. The frequency response of the filter can be obtained from a conveniently chosen set of its samples on a $N_1 \times N_2$ grid. For example,

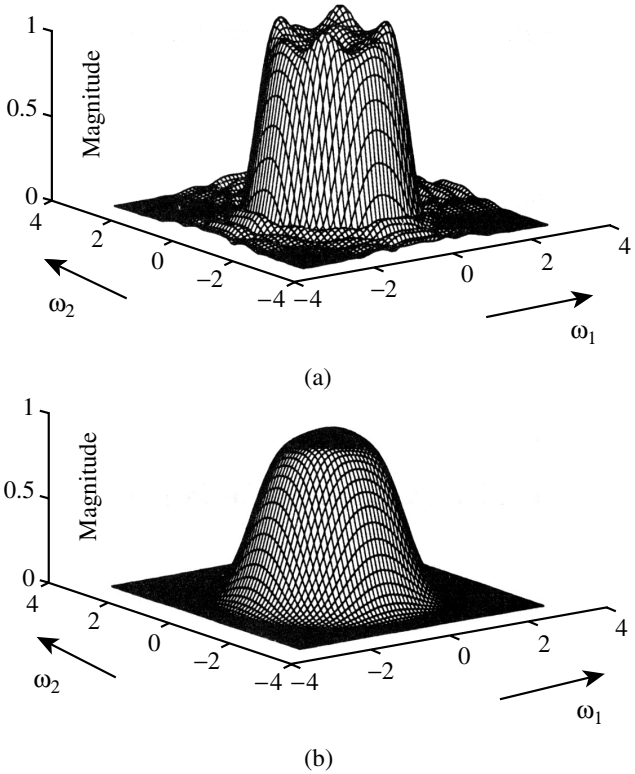

FIGURE 91.4 Frequency responses of the 2-D filters designed with (a) a rectangular window and (b) a separable window of Fig. 91.3(a).

the DFT of the impulse response can be used to interpolate the response for the entire region $[0,2\pi] \times [0,2\pi]$. The filter design then becomes a problem of choosing an appropriate set of DFT coefficients [21].

One choice of DFT coefficients consists of the ideal frequency response values, assuming a suitable cutoff. However, the resultant filters usually exhibit large magnitude deviations away from the DFT sample locations in the filter passbands and stopbands. The approximation error can be reduced by allowing the DFT values in the transition band to vary, and choosing them to minimize the deviation of the magnitude from the desired values. Another option is to allow all the DFT values to vary, and pick the optimal set of values for minimum error. The use of DFT-based interpolation allows for a computationally efficient implementation. The implementation cost of the method basically consists of a 2-D array product and inverse discrete Fourier transform (IDFT) computation, with appropriate addition.

Let us consider the set $S \subset Z^2$ that defines the equi-spaced frequency locations $\left(\frac{2k_1\pi}{N_1}, \frac{2k_2\pi}{N_2}\right)$:

$$S = \{k_1 = 0,1,...,N_1 - 1, k_2 = 0,1,...,N_2 - 1\}. \tag{91.18}$$

The DFT values can be expressed as

$$H_{DFT}[k_1,k_2] = H(\omega_1,\omega_2)\Big|_{(\omega_1,\omega_2)=\left(\frac{2k_1\pi}{N_1},\frac{2k_2\pi}{N_2}\right)}, \ (k_1,k_2) \in S. \tag{91.19}$$

The filter coefficients, $h(n_1, n_2)$, are found by using an IDFT computation

$$h(n_1,n_2) = \frac{1}{N_1N_2}\sum_{k_1=0}^{N_1-1}\sum_{k_2=0}^{N_2-1} H_{DFT}[k_1,k_2]e^{j\left(\frac{2\pi}{N_1}k_1n_1+\frac{2\pi}{N_2}k_2n_2\right)}, \ (n_1,n_2) \in S. \tag{91.20}$$

If Eq. (91.20) is substituted in the the expression for frequency response

$$H(\omega_1,\omega_2)=\sum_{n_1=0}^{N_1-1}\sum_{n_2=0}^{N_2-1}h(n_1,n_2)e^{-j(\omega_1 n_1+\omega_2 n_2)}, \tag{91.21}$$

we arrive at the interpolation formula

$$H(\omega_1,\omega_2)=\sum_{k_1=0}^{N_1-1}\sum_{k_2=0}^{N_2-1}H_{DFT}[k_1,k_2]A_{k_1k_2}(\omega_1,\omega_2), \tag{91.22}$$

where

$$A_{k_1k_2}(\omega_1,\omega_2)=\frac{1}{N_1N_2}\left(\frac{1-e^{-jN_1\omega_1}}{1-e^{-j(\omega_1-2\pi k_1/N_1)}}\right)\left(\frac{1-e^{-jN_2\omega_2}}{1-e^{-j(\omega_2-2\pi k_1k_2/N_2)}}\right). \tag{91.23}$$

Equation (91.22) serves as the basis of the frequency sampling design. As mentioned before, if the H_{DFT} are chosen directly according to the ideal response, then the magnitude deviations are usually large. To reduce the ripples, one option is to express the set S as the disjoint union of two sets S_t and S_c, where S_t contains indices corresponding to the transition band F_t, and S_c contains indices corresponding to the "care"-bands, i.e., the union of the passbands and stopbands, $F_p \cup F_s$. The expression for frequency response in Eq. (91.22) can be split into two summations, one over S_t and the other over S_c

$$H(\omega_1,\omega_2)=\sum_{S_t}H_{DFT}[k_1,k_2]A_{k_1k_2}(\omega_1,\omega_2)+\sum_{S_c}H_{DFT}[k_1,k_2]A_{k_1k_2}(\omega_1,\omega_2), \tag{91.24}$$

where the first term on the right-hand side is optimized. The design equations can be put in the form:

$$1-\alpha\delta\le H(\omega_1,\omega_2)\le 1+\alpha\delta,\ (\omega_1,\omega_2)\in F_p \tag{91.25}$$

and

$$-\delta\le H(\omega_1,\omega_2)\le \delta,\ (\omega_1,\omega_2)\in F_s \tag{91.26}$$

where δ is the peak approximation error in the stopband and $\alpha\delta$ is the peak approximation error in the passband, where α is any positive constant defining the relative weights of the deviations. The problem is readily cast as a linear programming problem with a sufficiently dense grid of points.

For equiripple design, all the DFT values H_{DFT} over S_t and S_c are allowed to vary. Following is an example of this design.

***Example*:** The magnitude response for the approximation of a circularly symmetric response is shown in Fig. 91.5. Here the passband is the interior of the circle $R_1 = \pi/3$ and the stopband is the exterior of the circle $R_2 = 2\pi/3$. With $N_1 = N_2 = 9$, the passband ripple is 0.08dB and the minimum stopband attenuation is 32.5dB.

FIR Filters Optimal in L_p Norm

A criterion different from the minimax criterion is briefly examined. Let us define the error at the frequency pair (ω_1, ω_2) as follows:

$$E(\omega_1,\omega_2)=H(\omega_1,\omega_2)-H_{id}(\omega_1,\omega_2). \tag{91.27}$$

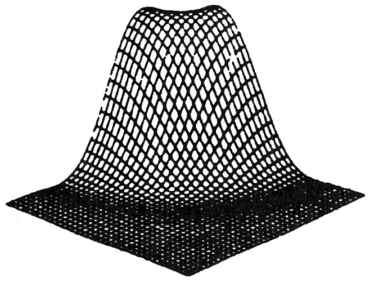

$R_1 = 1.5\pi/4.5$
$R_2 = 3\pi/4.5$
$N_1 = N_2 = 9$
AMPLITUDE RESPONSE

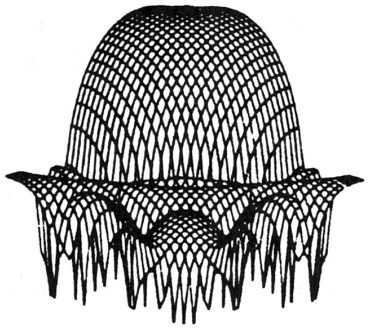

LOG MAGNITUDE RESPONSE
IN-BAND RIPPLE = 0.08
PEAK ATTENUATION = 32.5dB

FIGURE 91.5 Frequency response of the circularly symmetric filter obtained by using the frequency sampling method. (Adaped from [23] with permission from IEEE.)

One design approach is to minimize the L_p norm of the error

$$\varepsilon_p = \left(\frac{1}{4\pi^2} \int_{-\pi}^{\pi} \int_{-\pi}^{\pi} \left| E(\omega_1, \omega_2) \right|^p d\omega_1 d\omega_2 \right)^{\frac{1}{p}}. \tag{91.28}$$

Filter coefficients are selected by a suitable algorithm. For $p = 2$ Parseval's relation implies that

$$\varepsilon_2^2 = \sum_{n_1=-\infty}^{\infty} \sum_{n_2=-\infty}^{\infty} \left[h(n_1, n_2) - h_{id}(n_1, n_2) \right]^2. \tag{91.29}$$

By minimizing (91.29) with respect to the filter coefficients, $h(n_1, n_2)$, which are nonzero only in a finite-extent region, I, one gets

$$h(n_1, n_2) = \begin{cases} h_{id}(n_1, n_2) & (n_1, n_2) \in I, \\ 0, & \text{otherwise.} \end{cases} \tag{91.30}$$

which is the filter designed by using a straightforward rectangular window. Due to the Gibbs phenomenon it may have large variations at the edges of passband and stopband regions. A suitable weighting function can be used to reduce the ripple [2], and an approximately equiripple solution can be obtained.

For the general case of $p \neq 2$ [32], the minimization of (91.28) is a nonlinear optimization problem. The integral in (91.28) is discretized and minimized by using an iterative nonlinear optimization technique. The solution for $p = 2$ is easy to obtain using linear equations. This serves as an excellent initial estimate for the coefficients in the case of larger values of p. As p increases, the solution becomes approximately equiripple. The error term, $E(\omega_1, \omega_2)$, in (91.28) is nonuniformly weighted in passbands and stopbands, with larger weight given close to band-edges where deviations are typically larger.

Iterative Method for Approximate Minimax Design

We now consider a simple procedure based on alternating projections in the sample and frequency domains, which leads to an approximately equiripple response. In this method the zero-phase FIR filter design problem is formulated to alternately satisfy the frequency domain constraints on the magnitude response bounds and spatial domain constraints on the impulse response support [11, 12]. The algorithm is iterative and each iteration requires two 2-D FFT computations.

As pointed out in Section 91.2, 2-D FIR filter specifications are given as requirements on the magnitude response of the filter. It is desirable that the frequency response, $H(\omega_1, \omega_2)$, of the zero-phase FIR filter be within prescribed upper and lower bounds in its passbands and stopbands. Let us specify bounds on the frequency response $H(\omega_1, \omega_2)$ of the minimax FIR filter, $h\ (n_1, n_2)$, as follows

$$H_{id}(\omega_1,\omega_2) - E_d(\omega_1,\omega_2) \le H(\omega_1,\omega_2) \le H_{id}(\omega_1,\omega_2) + E_d(\omega_1,\omega_2)\ \omega_1,\omega_2 \in R, \tag{91.31}$$

where $H_{id}(\omega_1, \omega_2)$ is the ideal filter response, $E_d(\omega_1, \omega_2)$ is a positive function of (ω_1, ω_2) which may take different values in different passbands and stopbands, and R is a region defined in (91.28) consisting of passbands and stopbands of the filter (note that $H(\omega_1, \omega_2)$ is real for a zero-phase filter). Usually, $E_d(\omega_1, \omega_2)$ is chosen constant in a passband or a stopband. Inequality (91.31) is the frequency domain constraint of the iterative filter design method.

In spatial domain the filter must have a finite-extent support, I, which is symmetric region around the origin. The spatial domain constraint requires that the filter coefficients must be equal to zero outside the region, I.

The iterative method begins with an arbitrary finite-extent, real sequence $h_0(n_1, n_2)$ that is symmetric ($h_0\ (n_1, n_2) = h_0\ (-n_1, n_2)$). Each iteration consists of making successive imposition of spatial and frequency domain constraints onto the current iterate. The kth iteration consists of the following steps:

- Compute the Fourier transform of the kth iterate $h_k(n_1, n_2)$ on a suitable grid of frequencies by using a 2-D FFT algorithm.
- Impose the frequency domain constraint as follows:

$$G_k(\omega_1,\omega_2) = \begin{cases} H_{id}(\omega_1,\omega_2) + E_d(\omega_1,\omega_2) & \text{if } H_k(\omega_1,\omega_2) > H_{id}(\omega_1,\omega_2) + E_d(\omega_1,\omega_2), \\ H_{id}(\omega_1,\omega_2) - E_d(\omega_1,\omega_2) & \text{if } H_k(\omega_1,\omega_2) < H_{id}(\omega_1,\omega_2) - E_d(\omega_1,\omega_2), \\ H_k(\omega_1,\omega_2) & \text{otherwise.} \end{cases} \tag{91.32}$$

- Compute the inverse Fourier transform of $G_k(\omega_1, \omega_2)$.
- Zero out $g_k(n_1, n_2)$ outside the region I to obtain h_{k+1}.

The flow diagram of this method is shown in Fig. 91.6. It can be proven that the algorithm converges for all symmetric input sequences. This method requires the specification of the bounds or equivalently, $E_d(\omega_1, \omega_2)$, and the filter support, I. In 2-D filter design, filter order estimates for prescribed frequency domain specifications are not available. Therefore, successive reduction of bounds is used. If the specifications are too tight, then the algorithm does not converge. In such cases one can either progressively enlarge the filter support region, or relax the bounds on the ideal frequency response.

The size of the 2-D FFT must be chosen sufficiently large. The passband and stopband edges are very important for the convergence of the algorithm. These edges must be represented accurately on the frequency grid of the FFT algorithm.

The shape of the filter support is very important in any 2-D filter design method. The support should be chosen to exploit the symmetries in the desired frequency response. For example, diamond-shaped supports show a clear advantage over the commonly assumed rectangular regions in designing diamond filters or 90° fan filters [4, 6].

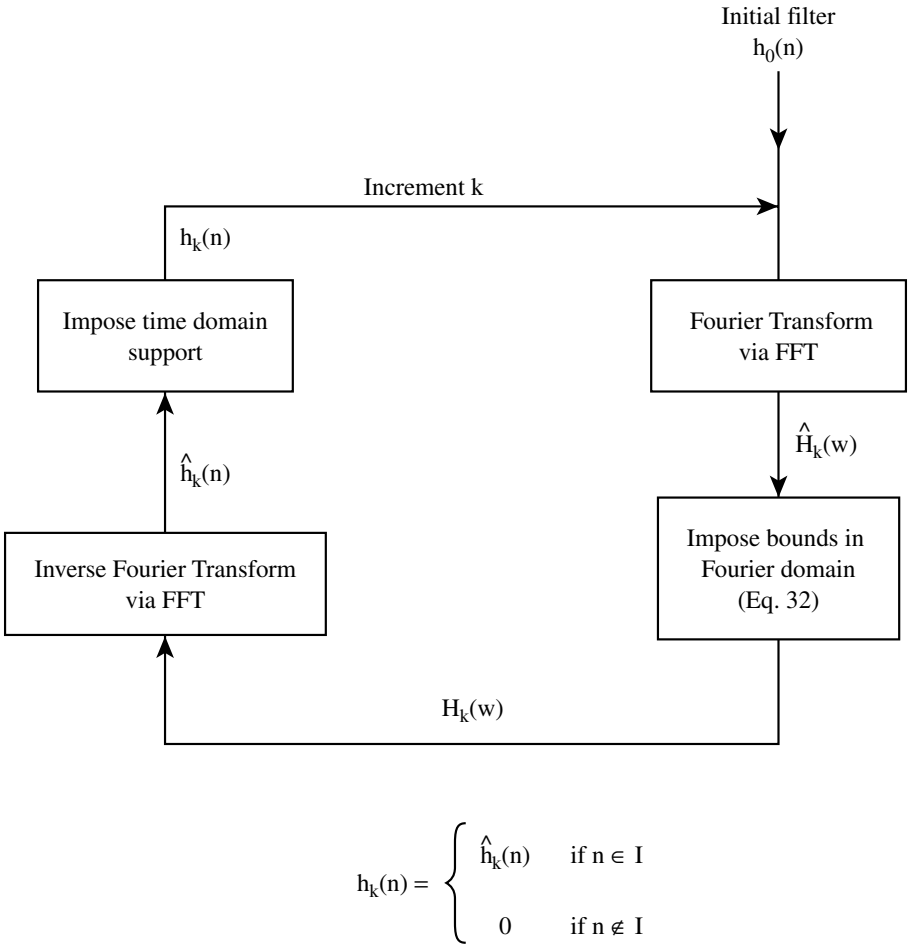

FIGURE 91.6 Flow diagram of the iterative filter design algorithm.

Since there are efficient FFT routines, 2-D FIR filters with large orders can be designed by using this procedure.

Example 1: Let us consider the design of a circularly symmetric lowpass filter. Maximum allowable deviation is $\delta_p = \delta_s = 0.05$ in both passband and the stopband. The passband and stopband cut-off boundaries have radii of $0.43\,\pi$ and $0.63\,\pi$, respectively. This means that the functions $E_d(\omega_1, \omega_2) = 0.05$ in the passband and the stopband. In the transition band the frequency response is conveniently bounded by the lower bound of the stopband and the upper bound of the passband. The filter support is a square shaped 17×17 region. The frequency response of this filter is shown in Fig. 91.7.

Example 2: Let us now consider an example in which we observe the importance of filter support. We design a fan filter whose specifications are shown in Fig. 91.8. Maximum allowable deviation is $\delta_p = \delta_s = 0.1$ in both passband and the stopband. If one uses a 7×7 square-shaped support which has 49 points, then it cannot meet the design specifications. However, a diamond shaped support,

$$I_d = \{-5 \le n_1 + n_2 \le 5\} \cap \{-5 \le n_1 - n_2 \le 5\}, \tag{91.33}$$

together with the restriction that

$$I_{de} = I_d \cap \{n_1 + n_2 = \text{odd or } n_1 = n_2 = 0\} \tag{91.34}$$

produces a filter satisfying the bounds. The filter support region, I_{de}, contains 37 points. The resultant frequency response is shown in Fig. 91.8.

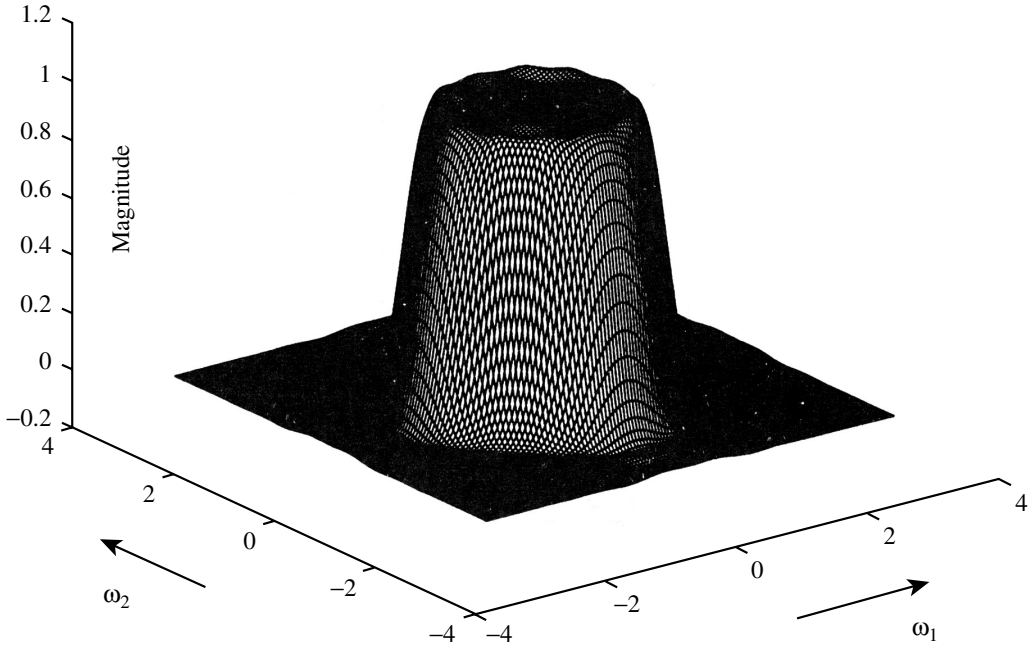

(a)

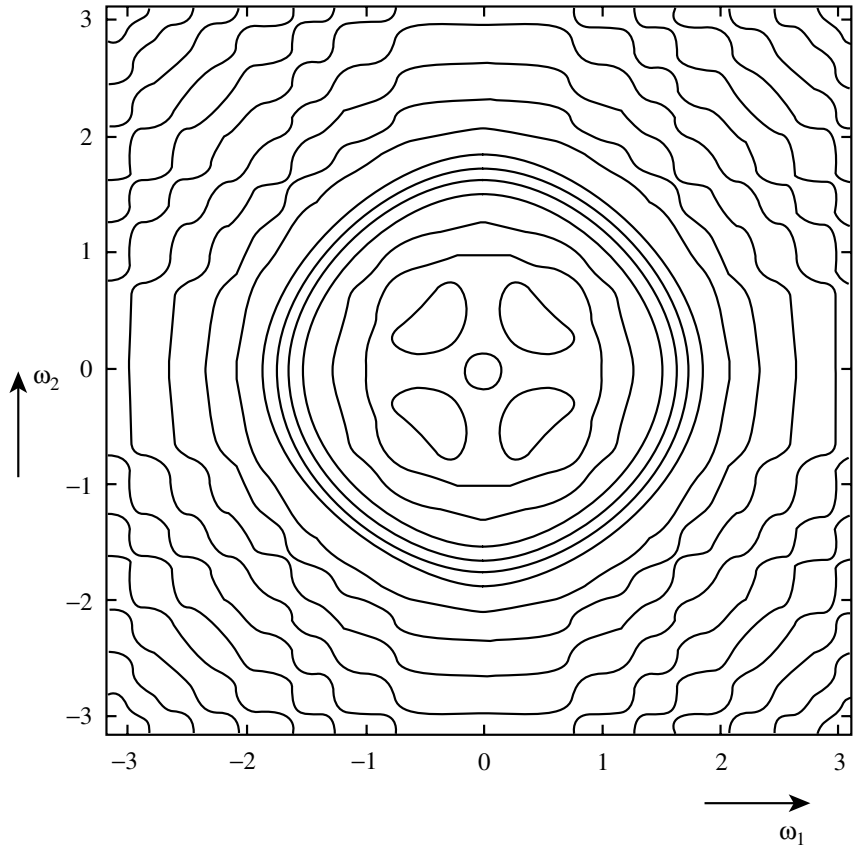

(b)

FIGURE 91.7 (a) Frequency response and (b) contour plot of the lowpass filter of Example 1.

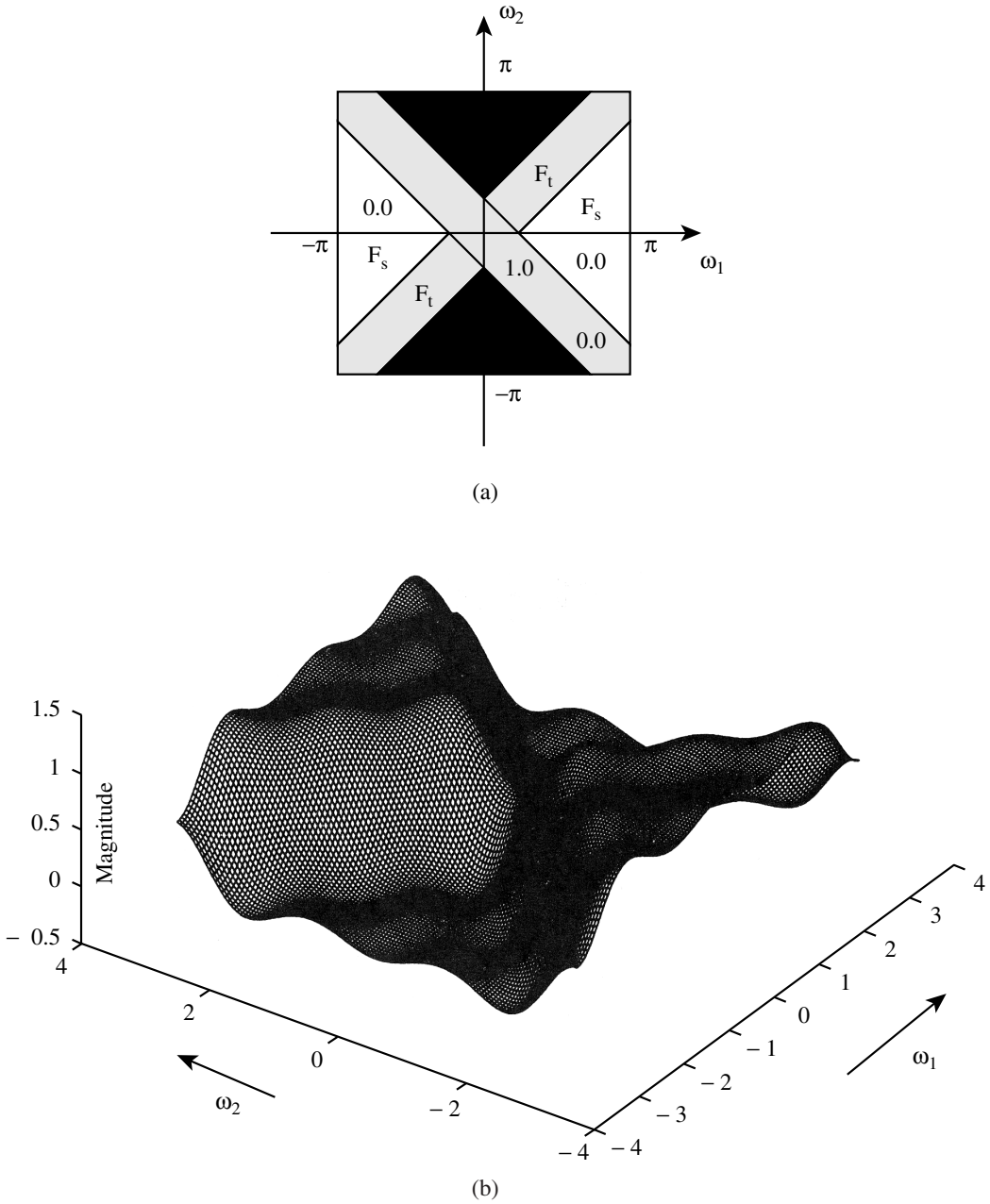

FIGURE 91.8 (a) Specifications and (b) perspective frequency response of the fan filter designed in Example 2.

91.4 Special Design Procedure for Restricted Classes

Many cases of practical importance typically require filters belonging to restricted classes. The stopbands and passbands of these filters are often defined by straight-line, circular or elliptical boundaries. In these cases, specialized procedures lead to efficient design and low-cost implementation. The filters in these cases are derived from 1-D prototypes.

Separable 2-D FIR Filter Design

The design of 2-D FIR filters composed of 1-D building blocks is briefly discussed. In cases where the specifications are given in terms of multiple passbands in the shapes of rectangles with sides parallel to the frequency axes, the design problem can be decomposed into multiple designs. The resulting filter is a parallel connection of component filters that are themselves separable filters. The separable structure was encountered earlier in the construction of 2-D windows from 1-D windows in Section 91.3. The

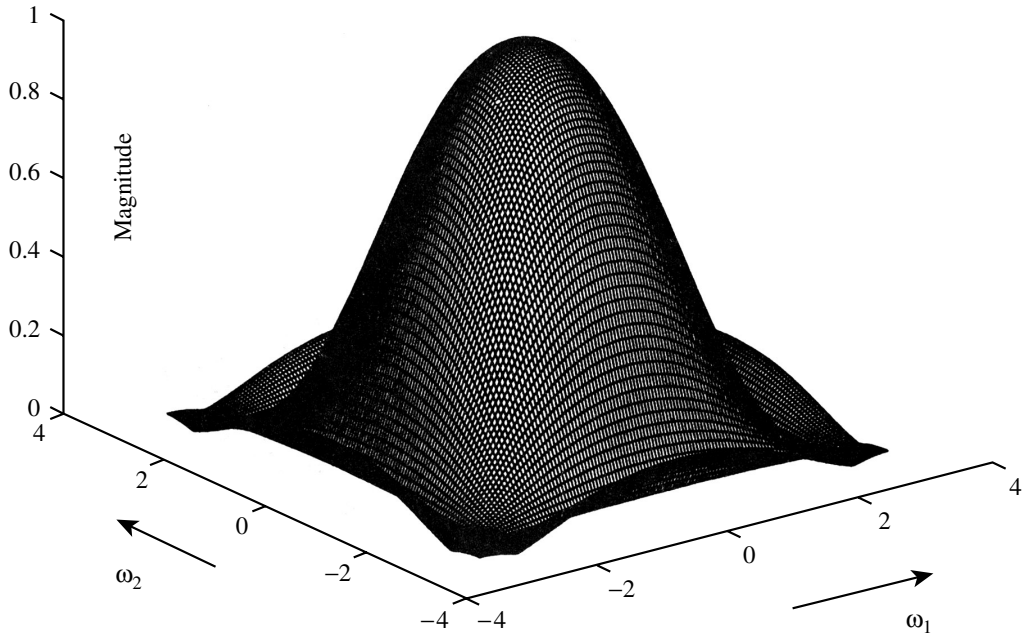

FIGURE 91.9 Frequency response of the separable lowpass filter $H(\omega_1, \omega_2) = H_1(\omega_1)H_1(\omega_2)$ where $H_1(\omega)$ is a 7th order Lagrange filter.

design approach is essentially the same. We will confine the discussion to cascade structures, which is a simple and very important practical case.

The frequency response of the 2-D separable FIR filter is expressed as

$$H(\omega_1, \omega_2) = H_1(\omega_1)H_2(\omega_2), \tag{91.35}$$

where $H_1(\omega)$ and $H_2(\omega)$ are frequency responses of two 1-D zero-phase FIR filters of durations N_1 and N_2. The corresponding 2-D filter is also a zero-phase FIR filter with $N \times M$ coefficients, and its impulse response is given by

$$h(n_1, n_2) = h_1(n_1)h_2(n_2), \tag{91.36}$$

where $h_1(n)$ and the $h_2(n)$ are the impulse responses of the 1-D FIR filters.

If the ideal frequency response can be expressed in a separable cascade form as in (91.35), then the design problem is reduced to the case of appropriate 1-D filter designs. A simple but important example is the design of a 2-D low-pass filter with a symmetric square-shaped passband, $PB = \{(\omega_1, \omega_2): |\omega_1| < \omega_c, |\omega_2| < \omega_c\}$. Such a lowpass filter can be designed from a single 1-D FIR filter with a cut-off frequency of ω_c by using (91.36). A lowpass filter constructed this way is used in Fig. 91.2(c). The frequency response of this 2-D filter whose 1-D prototypes are 7th order Lagrange filters is shown in Fig. 91.9.

This design method is also used in designing 2-D filter banks which are utilized in subband coding of images and video signals [49, 51, 52]). The design of 2-D filter banks is discussed in Section 91.6.

Frequency Transformation Method

In this method a 2-D zero-phase FIR filter is designed from a 1-D zero-phase filter by a clever substitution of variables. The design procedure was first proposed by McClellan [33] and the frequency transformation is usually called the McClellan transformation [14, 37, 35, 38].

Let $H_1(\omega)$ be the frequency response of a 1-D zero-phase filter with $2N+1$ coefficients. The key idea of this method is to find a suitable transformation $\omega = G(\omega_1, \omega_2)$ such that the 2-D frequency response, $H(\omega_1, \omega_2)$, which is given by

$$H(\omega_1,\omega_2) = H_1(\omega)\Big|_{\omega=G(\omega_1,\omega_2)} \tag{91.37}$$

approximates the desired frequency response, $H_{id}(\omega_1, \omega_2)$.

Since the 1-D filter is a zero-phase filter, its frequency response is real, and it can be written as follows:

$$H_1(\omega) = h_1(0) + \sum_{n=1}^{N} 2h_1(n)\cos(\omega n), \tag{91.38}$$

where the term $\cos(\omega n)$ can be expressed as a function of $\cos(\omega)$ by using the nth order Chebyshev polynomial, T_n,[2] i.e.,

$$\cos(\omega n) = T_n(\cos(\omega)). \tag{91.39}$$

Using (91.39), the 1-D frequency response can be written as

$$H_1(\omega) = \sum_{n=0}^{N} 2b(n)(\cos(\omega))^n, \tag{91.40}$$

where the coefficients, $b(n)$, are related to the filter coefficients, $h(n)$.

In this design method the key step is to substitute a transformation function, $F(\omega_1, \omega_2)$, for $\cos(\omega)$ in (91.40). In other words, the 2-D frequency response, $H(\omega_1, \omega_2)$, is obtained as follows:

$$\begin{aligned} H(\omega_1,\omega_2) &= H_1(\omega)\big|_{\cos(\omega)=F(\omega_1,\omega_2)} \\ &= \sum_{n=0}^{N} 2b(n)(F(\omega_1,\omega_2))^n. \end{aligned} \tag{91.41}$$

The function, $F(\omega_1, \omega_2)$, is called the McClellan transformation.

The frequency response, $H(\omega_1, \omega_2)$, of the 2-D FIR filter is determined by two free functions, the 1-D prototype frequency response, $H_1(\omega)$, and the transformation, $F(\omega_1, \omega_2)$. In order to have $H(\omega_1, \omega_2)$ be the frequency response of an FIR filter, the transformation, $F(\omega_1, \omega_2)$, must itself be the frequency response of a 2-D FIR filter. McClellan proposed $F(\omega_1, \omega_2)$ to be the frequency response of a 3×3 zero-phase filter in [33]. In this case the transformation, $F(\omega_1, \omega_2)$, can be written as follows:

$$F(\omega_1,\omega_2) = A + B\cos(\omega_1) + C\cos(\omega_2) + D\cos(\omega_1-\omega_2) + E\cos(\omega_1+\omega_2), \tag{91.42}$$

where the real parameters, A, B, C, D, and E, are related to the coefficients of the 3×3 zero-phase FIR filter. For $A = -\frac{1}{2}$, $B = C = \frac{1}{2}$, $D = E = \frac{1}{4}$, the contour plot of the transformation, $F(\omega_1, \omega_2)$, is shown in Fig. 91.10. Note that in this case the contours are approximately circularly symmetric around the origin. It can be seen that the deviation from the circularity, expressed as a fraction of the radius, decreases with the radius. In other words, the distortion from a circular response is larger for large radii. It is observed from Fig. 91.10 that, with the above choice of parameters, A, B, C, D, and E, the transformation is bounded ($|F(\omega_1, \omega_2)| \le 1$), which implies that $H(\omega_1, \omega_2)$ can take only the values that are taken by the 1-D prototype filter, $H_1(\omega)$. Since $|\cos(\omega)| \le 1$, the transformation, $F(\omega_1, \omega_2)$, which replaces $\cos(\omega)$ in (19.41) must also take values between 1 and –1. If a particular transformation does not obey these bounds, then it can be scaled such that the scaled transformation satisfies the bounds.

[2]Chebyshev polynomials are recursively defined as follows: $T_0(x) = 1$, $T_1(x) = x$, and $T_n(x) = 2xT_{n-1}(x) - T_{n-2}(x)$.

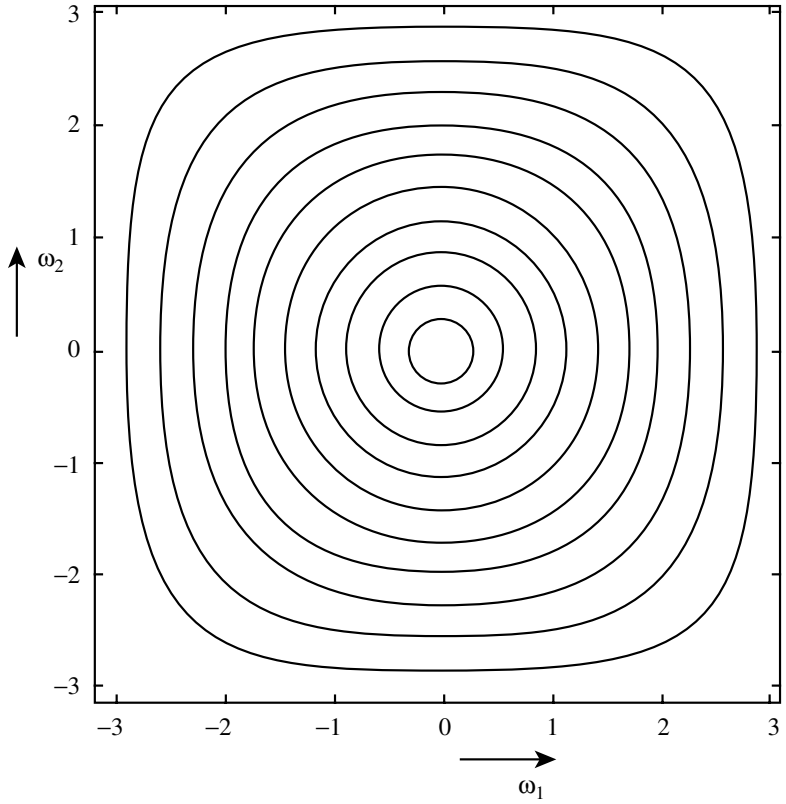

FIGURE 91.10 Contour plot of the McClellan transformation, $F(\omega_1, \omega_2) = 0.5\cos(\omega_1) + 0.5\cos(\omega_2) + 0.5\cos(\omega_1)\cos(\omega_2) - 0.5$.

If the transformation, $F(\omega_1, \omega_2)$, is real (it is real in (19.42)) then the 2-D filter, $H(\omega_1, \omega_2)$, will also be real or, in other words, it will be a zero-phase filter. Furthermore, it can be shown that the 2-D filter, $H(\omega_1, \omega_2)$, is an FIR filter with a support containing $(2M_1N + 1) \times (2M_2N + 1)$ coefficients, if the transformation, $F(\omega_1, \omega_2)$, is an FIR filter with $(2M_1 + 1) \times (2M_2 + 1)$ coefficients, and the order of the 1-D prototype filter is $2N + 1$. In (19.42) $M_1 = M_2 = 1$. As it can be intuitively guessed, one can design a 2-D approximately circularly symmetric low-pass (highpass) [bandpass] filter with the above McClellan transformation by choosing the 1-D prototype filter, $H_1(\omega)$, a low-pass (highpass) [bandpass] filter.

We will present some examples to demonstrate the effectiveness of the McClellan transformation.

Example 1: 2-D Window Design by Transformations [53]: In this example we design 2-D windows by using the McClellan transformation. Actually, we briefly mentioned this technique in Section 91.3. The 1-D prototype filter is chosen as an arbitrary 1-D symmetric window centered at the origin. Let $w(n)$ be the 1-D window of size $2N + 1$, and $W(\omega) = \sum_{n=-N}^{N} w(n)\exp(-j\omega n)$ be its frequency response. The transformation, $F(\omega_1, \omega_2)$, is chosen as in (91.42) with the parameters $A = -\frac{1}{2}$, $B = C = \frac{1}{2}$, $D = E = \frac{1}{4}$, of Fig. 91.10. This transformation, $F(\omega_1, \omega_2)$, can be shown to be equal to

$$F(\omega_1, \omega_2) = 0.5\cos(\omega_1) + 0.5\cos(\omega_2) + 0.5\cos(\omega_1)\cos(\omega_2) - 0.5. \tag{91.43}$$

The frequency response of the McClellan window, $H_t(\omega_1, \omega_2)$, is given by

$$H_t(\omega_1, \omega_2) = W(\omega)\Big|_{\cos(\omega)=F(\omega_1,\omega_2)}. \tag{91.44}$$

The resultant 2-D zero-phase window, $w_t(n_1, n_2)$, is centered at the origin and of size $(2N + 1) \times (2N + 1)$ because $M_1 = M_2 = 1$. The window coefficients can be computed either by using the inverse Chebyshev

relation,[3] or by using the inverse Fourier transform of (91.44). The frequency response of a 2-D window constructed from a 1-D Hamming window of order 13 is shown in Fig. 91.3(c). The size of the window is 13×13.

Example 2: Let us consider the design of a circularly symmetric lowpass filter and a bandpass filter by using the transformation of (91.43). In this case, if one starts with a 1-D lowpass (bandpass) filter as the prototype filter, then the resulting 2-D filter will be a 2-D circularly symmetric lowpass (bandpass) filter due to the almost circularly symmetric nature of the transformation. In this example, the Lagrange filter of order 7 considered in Section 91.2 is used as the prototype. The prototype 1-D bandpass filter of order 15 is designed by using the Parks-McClellan algorithm [41].

It is seen from the above examples that filters designed by the transformation method appear to have better frequency responses than those designed by the windowing or frequency sampling methods. In other words, one can control the 2-D frequency response by controlling the frequency response of the 1-D prototype filter and choosing a suitable 2-D transformation. Furthermore, in some special cases it was shown that minimax optimal filters can be designed by the transformation method [20].

We have considered specific cases of the special transformations given by (91.42). By varying the parameters in (91.42) or expanding the transformation to include additional terms, a wider class of contours can be approximated. Ideally, the frequency transformation approach requires the simultaneous optimal selection of the transformation, $F(\omega_1,\omega_2)$, and the 1-D prototype filter $H_1(\omega)$ to approximate a desired 2-D frequency response. This can be posed as a nonlinear optimization problem. However, a suboptimal two-stage design by separately choosing $F(\omega_1,\omega_2)$ and $H_1(\omega)$ works well in practice. The transformation $F(\omega_1,\omega_2)$ should approximate 1 (–1) in the passband (stopband) of the desired filter. The contour produced by the transformation corresponding to the 1-D passband (stopband) edge frequency, ω_p (ω_s), should ideally map to the given passband (stopband) boundary in the 2-D specifications. However, this cannot be achieved in general given the small number of variable parameters in the transformation. The parameters are therefore selected to minimize a suitable norm of the error between actual and ideal (constant) values of the transformation over the boundaries.

Various transformations and design considerations are described in [37, 38, 40, 43]. The use of this transformation in exact reconstruction filter bank design was proposed in [7].

Filters designed by the transformation method can be implemented in a computationally efficient manner [14, 30]. The key idea is to implement (91.41) instead of implementing the filter by using the direct convolution sum. By implementing the transformation, $F(\omega_1,\omega_2)$, which is an FIR filter of low-order, in a modular structure realizing (91.41) is more advantages than ordinary convolution sum [14, 34].

In the case of circular passband design, it was observed that for low order transformation, the transformation contours exhibit large deviations from circularity. A simple artifice to overcome this problem in approximating wideband responses is to use decimation of a 2-D narrowband filter impulse response [18]. The solution consists of transforming the specifications to an appropriate narrowband design, where the deviation from circularity is smaller. The narrow passband can be expanded by decimation while essentially preserving the circularity of the passband.

Design Using Nonrectangular Transformations and Sampling Rate Conversions

In some filter specifications the desired responses are characterized by ideal frequency responses in which passbands and stopbands are separated by straight-line boundaries that are not necessarily parallel to the frequency axes. Examples of these are the various kinds of fan filters [4, 15, 17, 27] and diamond-shaped filters [6, 48]. Other shapes with straight-line boundaries are also approximated [8, 9, 13, 29, 28, 50]. Several design methods applicable in such cases have been developed and these methods are usually based on transformations related to concepts of sampling rate conversions. Often alternate frequency

[3] $1 = T_0$, (x), $x = T_1(x) - T_0(x)$, $x^2 = \frac{1}{2}(t_0(x) + T_2(x))$, $x^3 = \frac{1}{4}(3T_1(x) + T_3(x))$ etc.

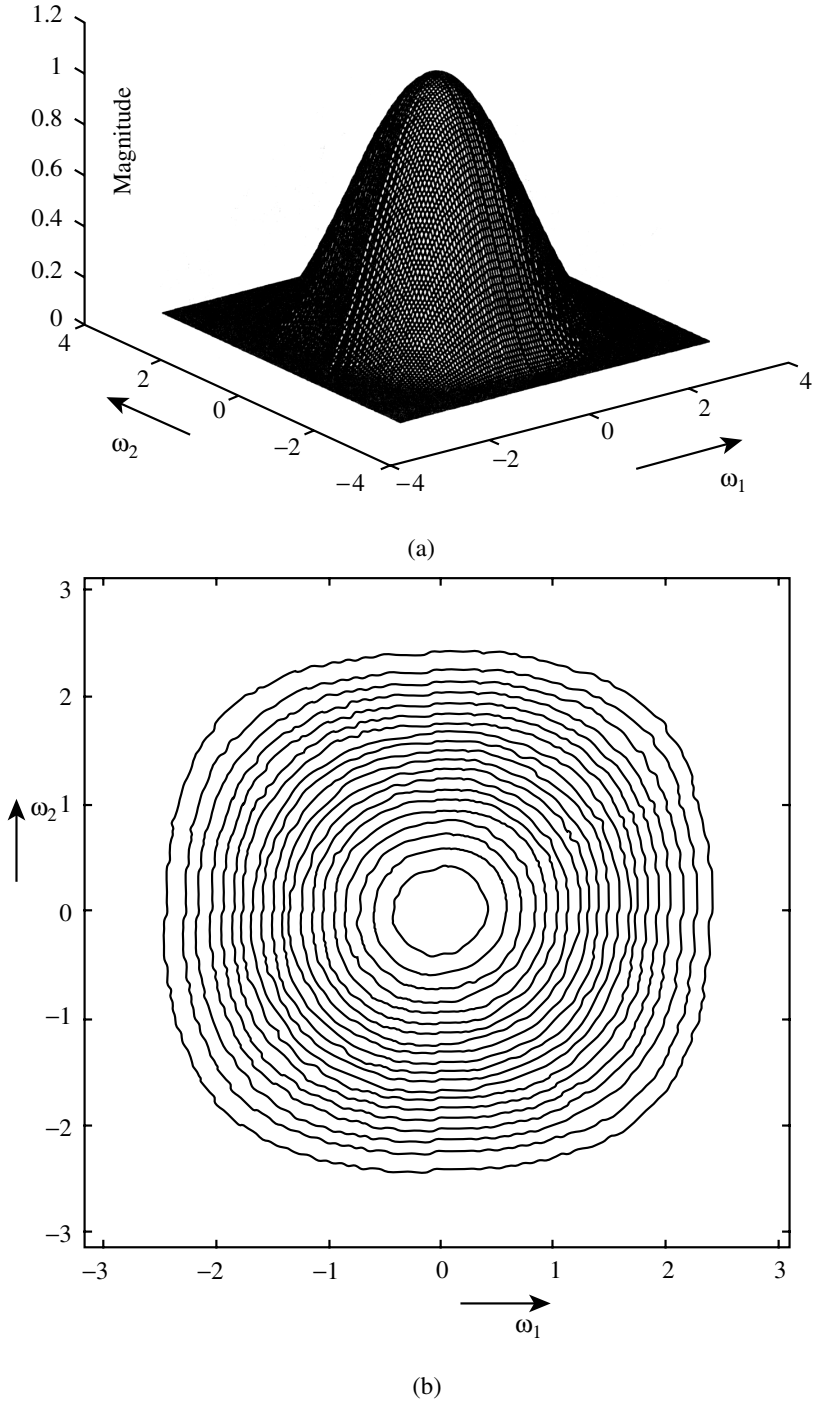

FIGURE 91.11 Frequency response and contour plots of the lowpass filter of Example 2.

domain interpretations are used to explain the design manipulations. A detailed treatment of these methods is beyond the scope of this chapter. However some key ideas are described, and a specific case of a diamond filter is used to illustrate the methods. The importance of these design methods stems from the implementation efficiency that results from a generalized notion of separable processing.

In the family of methods considered here, manipulations of a separable 2-D response using a combination of several steps is carried out. In the general case of designing filters with straight-line boundaries, it is difficult to describe a systematic procedure. However, in a given design problem, an appropriate set of steps in the design is suggested by the nature of the desired response.

Some underlying ideas can be understood by examining the problem of obtaining a filter with a parallellogram-shaped passband region. The sides of the parallellogram are assumed to be tilted with

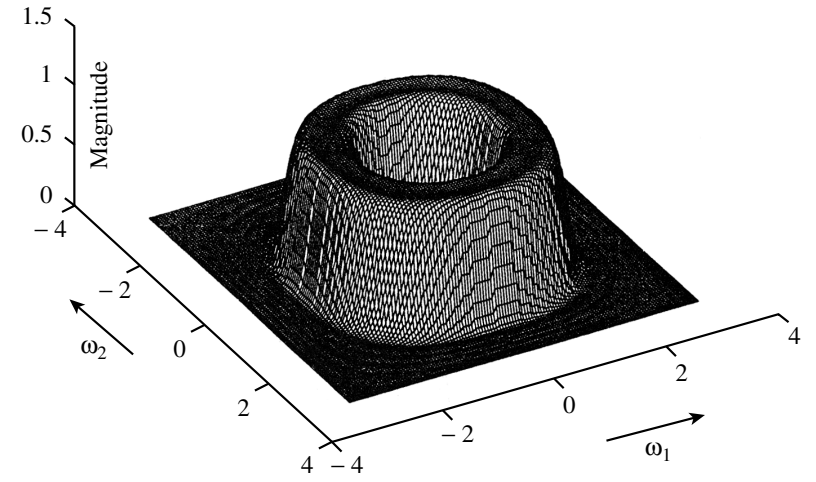

(a)

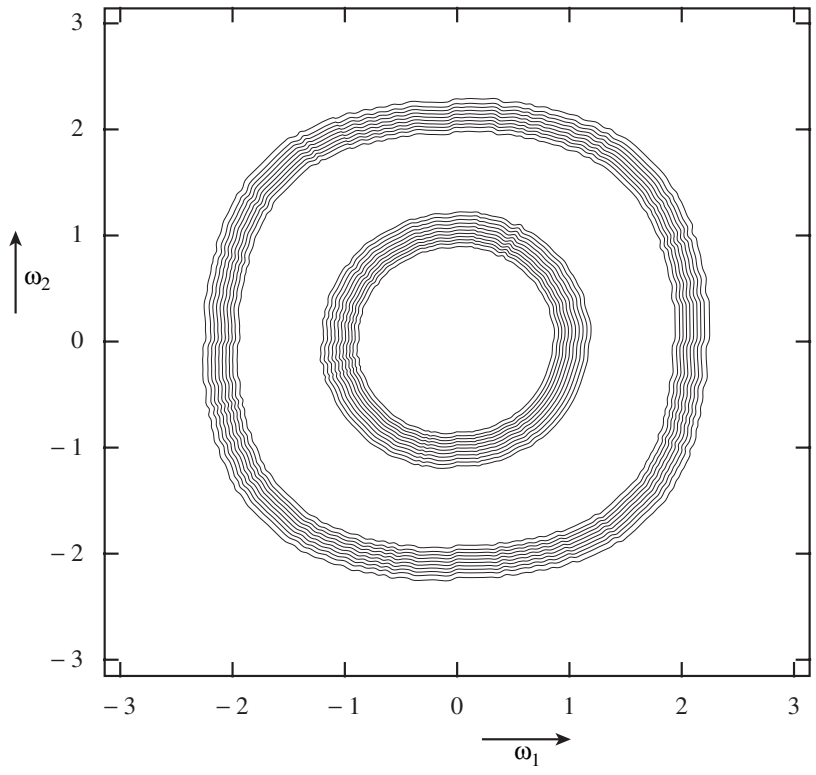

(b)

FIGURE 91.12 Frequency response and contour plots of the bandpass filter of Example 2.

respect to the frequency axes. One approach to solving this problem is to perform the following series of manipulations on a separable prototype filter with a rectangular passband. The prototype filter impulse response is upsampled on a *nonrectangular* grid. The upsampling is done by an integer factor greater than one and it is defined by a non-diagonal non-singular integer matrix [39]. The upsampling produces a parallellogram by a rotation and compression of the frequency response of the prototype filter together with a change in the periodicity. The matrix elements are chosen to produce the desired orientation in the resulting response. Depending on the desired response, cascading to eliminate unwanted portions of the passband in the frequency response, along with possible shifts and additions, may be used. The nonrectangular upsampling is then followed by a rectangular decimation of the sequence to expand the passband out to the desired size. In some cases the operations of the upsampling transformation and decimation can be combined by the use of nonrectangular decimation of impulse response samples.

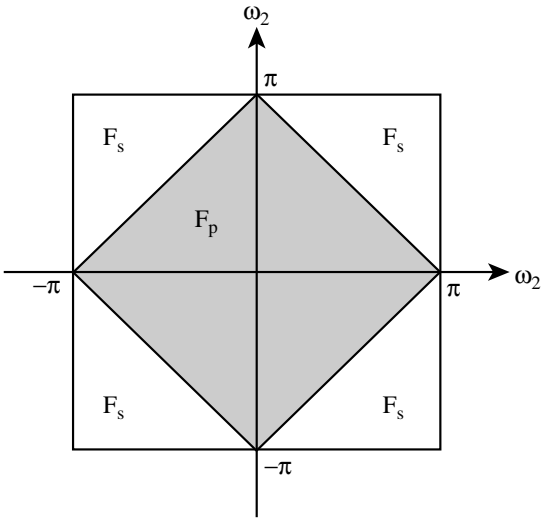

FIGURE 91.13 Ideal frequency respnse of a diamond filter.

Results using such procedures produce efficient filter structures that are implemented with essentially 1-D techniques but where the orientations of processing are not parallel to the sample coordinates.

Consider the case of a diamond filter design shown in Fig. 91.13. Note that the filter in Fig. 91.13 can be obtained from the filter in Fig. 91.14(a) by a transformation of variables. If $F_a(z_1, z_2)$ is the transfer function of the filter approximating the response in Fig. 91.14(a), then the diamond filter transfer function $D(z_1, z_2)$ given by

$$D(z_1, z_2) = F_a\left(z_1^{\frac{1}{2}} z_2^{\frac{1}{2}}, z_1^{-\frac{1}{2}} z_2^{\frac{1}{2}}\right) \tag{91.45}$$

will approximate the response in Fig. 91.1(a). The response in Fig. 91.2(a) can be expressed as the sum of the two responses shown in Fig. 91.2(b) and (c). We observe that if $F_b(z_1, z_2)$ is the transfer function of the filter approximating the response in Fig. 91.2(b) then

$$F_c(z_1, z_2) = F_b(-z_1, -z_2) \tag{91.46}$$

will approximate the response in Fig. 91.14(c). This is due to the fact that negating the arguments shifts the (periodic) frequency response of F_b by (π, π). The response in Fig. 91.14(b) can be expressed as the product of two ideal 1-D lowpass filters, one horizontal and one vertical, which have the response shown in Fig. 91.14(d). This 1-D frequency response can be approximated by a halfband filter. Such an approximation will produce a response in which the transition band straddles both sides of the cutoff frequency boundaries in Fig. 91.14(a). If we wish to constrain the transition band to lie within the boundaries of the diamond-shaped region in Fig. 91.13(a), then we should choose a 1-D filter whose stopband interval is $(\pi/2, \pi)$. Let $H(z)$ be the transfer function of the prototype 1-D lowpass filter approximating the response in Fig. 91.14(d) with a suitably chosen transition boundary. The transfer function $H(z)$ can be expressed as

$$H(z) = T_1(z^2) + zT_2(z^2). \tag{91.47}$$

The transfer function F_a is given by

$$F_a(z_1, z_2) = H(z_1)H(z_2) + H(-z_1)H(-z_2). \tag{91.48}$$

Combining (91.45), (91.47), and (91.48) we get

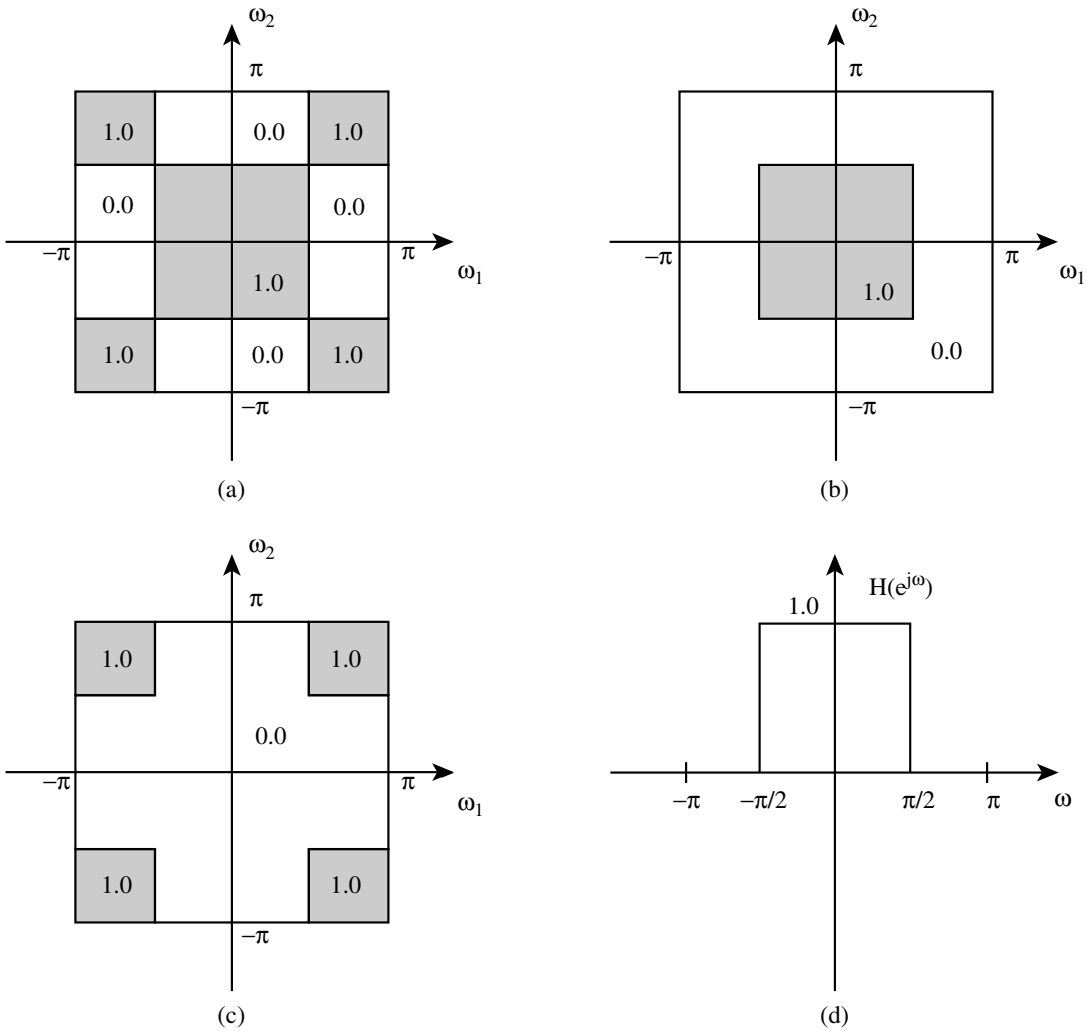

FIGURE 91.14 Ideal frequency responses of the filters (a) $F_a(z_1, z_2)$, (b) $F_b(-z_1, -z_2)$, (c) $F_c(z_1, z_2)$, and (d) $H(z)$ in obtaining a diamond filter.

$$D(z_1, z_2) = 2T_1(z_1, z_2)T_1(z_1^{-1}z_2) + 2z_2T_2(z_1, z_2)T_2(z_1^{-1}z_2). \tag{91.49}$$

As mentioned before, $H(z)$ can be chosen to be a halfband filter with

$$T_1(z^2) = 0.5. \tag{91.50}$$

The filter T_2 can be either FIR or IIR. It should be noted that the result can also be obtained as a nonrectangular downsampling, by a factor 2, of the impulse response of the filter $F_b(-z_1, -z_2)$.

Another approach that utilizes multirate concepts is based on a novel idea of applying frequency masking in the 2-D case [31].

91.5 2-D FIR Filter Implementation

The straightforward way to implement 2-D FIR filters is to evaluate the convolution sum given in (91.1). Let us assume that the FIR filter has L nonzero coefficients in its region of support I. In order to get an output sample, L multiplications and L additions need to be performed. The number of arithmetic operations can be reduced by taking advantage of the symmetry of the filter coefficients, that is, $h(n_1, n_2) = h(-n_1, -n_2)$. For example, let the filter support be a rectangular region, $I = \{n_1 = -N_1, \ldots, 0, 1, \ldots, N_1, n_2 = -N_2, \ldots, 0, 1, \ldots, N_2\}$. In this case,

$$y(n_1,n_2)=\sum_{k_1=-N_1}^{N_1}\sum_{k_2=1}^{N_2}\left[h(k_1,k_2)x(n_1-k_1,n_2-k_2)+x(n_1+k_1,n_2+k_2)\right]$$
$$+h(0,0)x(n_1,n_2)+\sum_{k_1=1}^{N_1}h(k_1,0)\left[x(n_1-k_1,n_2)+x(n_1+k_1,n_2)\right], \tag{91.51}$$

which requires approximately half of the multiplications required in the direct implementation (91.1). Any 2-D FIR filter can also be implemented by using an FFT algorithm. This is the direct generalization of 1-D FFT-based implementation [14, 30]. The number of arithmetic operations may be less than the space domain implementation in some cases.

Some 2-D filters have special structures that can be exploited during implementation. As we pointed out in Section 91.4, 2-D filters designed by McClellan-type transformations can be implemented in an efficient manner [14, 35, 34] by building a network whose basic module is the transformation function which is usually a low order 2-D FIR filter.

Two-dimensional FIR filters that have separable system responses can be implemented in a cascade structure. In general, an arbitrary 2-D polynomial cannot be factored into subpolynomials due to the absence of a counterpart of Fundamental Theorem of Algebra in two or higher dimensions (whereas in 1-D any polynomial can be factored into polynomials of lower orders). Since separable 2-D filters are constructed from 1-D polynomials, they can be factored and implemented in a cascade form. Let us consider (91.35) where $H(z_1,z_2)=H_1(z_1)H_2(z_2)$ which corresponds to $h(n_1, n_2) = h_1(n_1)\ h_2(n_2)$ in space domain. Let us assume that orders of the 1-D filters $h_1(n)$ and $h_2(n)$ are $2N_1+1$ and $2N_2+1$, respectively. In this case the 2-D filter, $h(n_1, n_2)$, has the same rectangular support, I, as in (91.51). Therefore,

$$y(n_1,n_2)=\sum_{k_2=-N_2}^{N_2}h_2(k_2)\sum_{k_1=-N_1}^{N_1}h(k_1)x(n_1-k_1,n_2-k_2). \tag{91.52}$$

The 2-D filtering operation in (91.52) is equivalent to a two-stage 1-D filtering in which the input image, $x(n_1, n_2)$, is first filtered horizontally line by line by $h_1(n)$, then the resulting output is filtered vertically column by column by $h_2(n)$. In order to produce an output sample, the direct implementation requires $(2N_1+1)\times(2N_2+1)$ multiplications, whereas the separable implementation requires $(2N_1 + 1) + (2N_2 + 1)$ multiplications, which is computationally much more efficient than the direct form realization. This is achieved at the expense of memory space (separable implementation needs a buffer to store the results of first stage during the implementation). By taking advantage of the symmetric nature of h_1 and h_2, the number of multiplications can be further reduced.

Filter design methods by imposing structural constraints like cascade, parallel, and other forms are proposed by several researchers including [47, 16]. These filters can be efficiently implemented because of their special structures. Unfortunately, the design procedure requires nonlinear optimization techniques which may be very complicated.

With advances in VLSI technology, the implementation of 2-D FIR filters using high-speed digital signal processors is becoming increasingly common in complex image processing systems.

91.6 Multi-Dimensional Filter Banks and Wavelets

Two-dimensional subband decomposition of signals using filter banks (that implement a 2-D wavelet transform) find applications in a wide range of tasks including image and video coding, restoration, denoising, and signal analysis. For example, in recently finalized JPEG-2000 image coding standard an image is first processed by a 2-D filter bank. Data compression is then carried out in the subband domain.

In most cases, 2-D filter banks are constructed in a separable form with the use of the filters of 1-D filter banks, i.e., as a product of two 1-D filters [49, 52]. We confine our attention to a 2-D four-channel

filter bank obtained from a 1-D two-channel filter bank. Let h_0 and h_1 denote the analysis filters of a 1-D two-channel filter bank. The four analysis filters of the separable 2-D filter bank are given by

$$h_{i,j}(n_1,n_2) = h_i(n_1)h_j(n_2), \quad i,\ j = 0,\ 1, \tag{91.53}$$

The filters h_0 and h_1 can be either FIR or IIR. If they are FIR (IIR), then the 2-D filters, $h_{i,j}$, are also FIR (IIR). Frequency responses of these four filters, $H_{i,j}(\omega_1,\omega_2)$, $i,j = 0,1$, are given by

$$H_{i,j}(\omega_1,\omega_2) = H_i(\omega_1)H_j(\omega_2), \quad i,\ j = 0,\ 1, \tag{91.54}$$

where $H_0(\omega_1)$ and $H_1(\omega_2)$ are the frequency responses of the 1-D low-pass (approximating an ideal cutoff frequency at $\pi/2$) and high-pass filters of a 1-D subband filter bank, respectively [51]. Any 1-D filter bank described in Chapter 89 can be used in (91.53) to design 2-D filter banks. Feature-rich structures for 1-D filter banks are described in [7, 8].

The 2-D signal is decomposed by partitioning its frequency domain support into four rectangular regions of equal areas. The ideal passband regions of the filters, $H_{i,j}(\omega_1,\omega_2)$, are shown in Fig. 91.15. For example, the ideal passband of $H_{0,0}(\omega_1,\omega_2)$ is the square region $[-\pi/2, \pi/2] \times [-\pi/2, \pi/2]$. The 2-D filter bank is shown in Fig. 91.16.

Corresponding 2-D synthesis filters are also constructed in a separable manner from the synthesis filters of the 1-D filter bank. If the 1-D filter bank has the perfect reconstruction (PR) property, then the 2-D filter bank also has the PR property. Subband decomposition filter banks (or filter banks implementing the 2-D wavelet transform) consist of analysis and synthesis filters, upsamplers, and downsamplers as discussed in Chapter 90. In the separable 2-D filter bank, downsampling is carried out both horizontally and vertically as follows:

$$x_0(n_1,n_2) = x_a(2n_1,2n_2) \tag{91.55}$$

Here we consider the input 2-D signal x_a to be an image. The downsampled image x_0 is a quarter-size version of x_a. Only one sample out of four is retained in the downsampling operation described in (91.55). The upsampling operation is the dual of the downsampling operation. In other words, a zero valued sample is inserted in upsampling corresponding to the location of each dropped sample during downsampling.

The implementation of the above filter bank can be carried out separably in a computationally efficient manner as described in Chapter 90 and [52, 49]. The input image is first processed horizontally row by

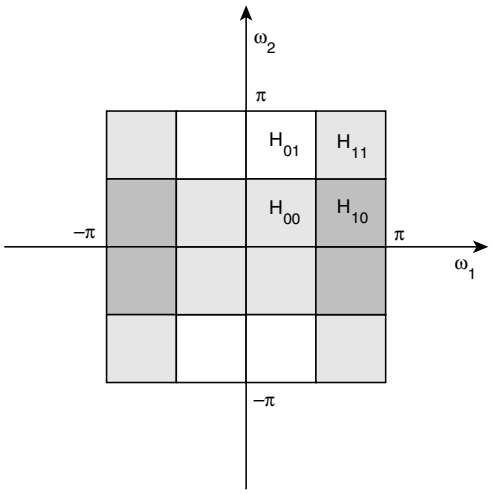

FIGURE 91.15 Ideal passband regions of the separable filters of a rectangular filter bank.

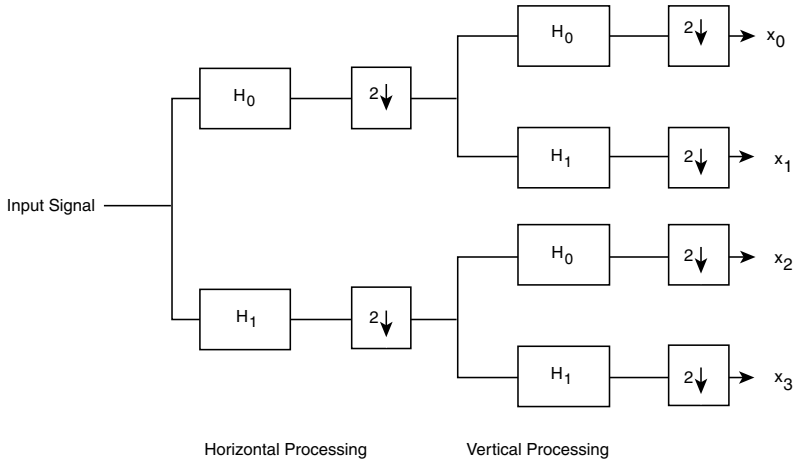

FIGURE 91.16 Block diagram of seperable processing in 2-D filter bank.

row by a 1-D filter bank with filters, h_0 and h_1. After the input signal is horizontally filtered with the 1-D two-channel filter bank, the signal in each channel is downsampled row-wise to yield two images. Each image is then filtered and downsampled vertically by the filter bank. As a result, four quarter-size subimages, x_i, i = 0, 1, 2, 3, are obtained. These images are the same as the images obtained by direct implementation of the analysis filter bank shown in Fig. 91.16. The synthesis filter bank is also implemented in a separable manner.

Nonseparable 2-D filter banks [14] are not as computationally efficient as separable filter banks as discussed in Section 91.5.

In two or higher dimensions, downsampling and upsampling are not restricted to the rectangular grid, but can be carried out in a variety of ways. One example of this is quincunx downsampling where the downsampled image x_q is related to the input image x_a as follows:

$$x_q(n_1,n_2) = x_a(n_1+n_2, n_2-n_1) \tag{91.56}$$

In this case only the samples for which n_1+ n_2 is even are retained in the output. Filter banks employing quincunx and other downsampling strategies are described in [5]-[7], [9], [50], [52]. Filter banks that employ quincunx downsampling have only two channels and the frequency support is partitioned in a diamond-shaped manner as shown in Fig. 91.13. Filters of a quincunx filter bank which have diamond-shaped passbands and stopbands can be designed from a 1-D subband decomposition filter bank using the transformation method described in Eqs. (91.45) through (91.48).

Acknowledgments

The authors would like to express their sincere thanks to Omer Nezih Gerek, Imad Abdel Hafez, and Ahmet Murat Bagci for the help they provided in preparing the figures for the chapter.

References

[1] A. Abo-Taleb and M. M. Fahmy "Design of FIR two-dimensional digital filters by successive projections," *IEEE Trans. Circuits and Systems,* vol. CAS-31, pp. 801-805, 1984.

[2] V. R. Algazi et al. *IEEE Trans. Circuits and Systems,* vol. CAS, 86.

[3] S. A. H. Aly and M. M. Fahmy, "Symmetry in two-dimensional rectangularly sampled digital filters," *IEEE Trans. Acoustics, Speech, and Signal Processing,* ASSP-29, pp. 794-805, 1981.

[4] R. Ansari, "Efficient IIR and FIR Fan Filters," *IEEE Trans. Circuits Syst.*, vol. CAS-34, pp. 941-945, August 1987.

[5] R. Ansari, A. E. Cetin and S. H. Lee, "Subband coding of images using nonrectangular filter banks," *Proc. of the SPIE 32nd Annual International Technical Symposium: Applications of Digital Signal Processing*, San Diego, CA, vol. 974, August 1988.

[6] R. Ansari, H. P. Gaggioni and D. J. Le Gall, "HDTV coding using a nonrectangular subband decomposition," *Proc. SPIE Conference on Visual Communications and Image Processing,* Boston, MA, vol. 1001, pp. 821-824, Nov. 1988.

[7] R. Ansari, "IIR filter banks and wavelets," in *Subband and Wavelet Transforms: Design and Applications*, M. J. T. Smith and A. N. Akansu, Eds., pp. 113-148, Norwell, MA: Kluwer Academic Publishers, 1996.

[8] R. Ansari, C. W. Kim, and M. Dedovic, "Structure and design of two-channel filter banks derived from a triplet of halfband filters," *IEEE Trans. on Circuits and Systems II*, vol. 46, pp. 1487-1496, Dec. 1999.

[9] R. Ansari and C. Guillemot, "Exact reconstruction filter banks using diamond FIR filters," *Proc.* 1990 *Bilkent Int. Conf. on New Trends in Comm., Control, and Signal Processing,* E. Arikan, Ed., pp. 1412- 1421, Elsevier, Holland, 1990.

[10] R. H. Bamberger and M. J. T. Smith, " Efficient 2-D analysis/synthesis filter banks for directional image component representation," *IEEE Int. Symposium on Circuits and Systems,* pp. 2009-2012, May 1990.

[11] R. H. Bamberger and M. J. T. Smith, "A filter bank for the directional decomposition of images: theory and design," *IEEE Trans. Acoust., Speech, Signal Processing,* pp. 882-892, April 1992.

[12] C. Charalambous, "The performance of an algorithm for minimax design of two-dimensional linear-phase FIR digital filters," *IEEE Trans. Circuits and Systems,* vol. CAS-32, pp. 1016-1028, 1985.

[13] A. E. Cetin and R. Ansari, "An iterative procedure for designing two dimensional FIR filters," *Proc. IEEE Int. Symposium on Circuits and Systems* (*ISCAS*), pp. 1044-1047, 1987.

[14] A. E. Cetin and R. Ansari, "Iterative procedure for designing two dimensional FIR filters", *Electronics Letters, IEE,* Vol. 23, pp. 131-133, Jan. 1987.

[15] T. Chen and P. P. Vaidyanathan, "Multidimensional multirate filters and filter banks derived from one-dimensional filters", *IEEE Trans. Signal Processing,* vol. 41, pp. 1035-1047, Mar. 1993.

[16] D. Dudgeon and R. M. Mersereau, *Multidimensional Digital Signal Processing*, Prentice-Hall, Englewood Cliffs, NJ, 1984.

[17] P. Embree, J. P. Burg, and M. M. Backus, "Wideband velocity filtering — The pie slice process", *Geophysics,* Vol. 28, pp. 948-974, 1963.

[18] O. D. Faugeras and J. F. Abramatic, "2-D FIR filter design from independent 'small' generating kernels using a mean square and Tchebyshev error criterion," *Proc. IEEE Int. Conf. Acoustics, Speech, and Signal Processing*, pp. 1-4, 1979.

[19] A. P. Gerheim, "Synthesis procedure for 90° fan filters," *IEEE Trans. Circuits and Systems,* vol. CAS-30, pp. 858-864, Dec. 1983.

[20] C. Guillemot and R. Ansari, "Two-dimensional filters with wideband circularly symmetric frequency response", *IEEE Trans. Circuits and Systems*.

[21] C. Guillemot, A. E. Cetin, and R. Ansari, "Nonrectangular wavelet representation of 2-D signals: application to image coding," *Wavelets and Application to Image Coding*, M. Barlaud, Ed., pp. 27-64, Amsterdam, Holland: Elsevier Publications, 1994.

[22] D. B. Harris and R. M. Mersereau, "A comparison of algorithms for minimax design of two-dimensional linear phase FIR digital filters," *IEEE Trans. Acoustics, Speech, and Signal Processing,* ASSP-25, pp. 492-500, 1977.

[23] J. V. Hu and L.R. Rabiner, "Design techniques for two-dimensional digital filters," *IEEE Trans. Audio Electroacoust.,* Vol. 20, pp. 249-257, 1972.

[24] T. S. Huang, "Two-dimensional windows," *IEEE Trans. Audio and Electroacoustics*, vol. AU-20, no. 1, pp. 88-90, 1972.

[25] T. S. Huang, Ed., *Two-Dimensional Digital Signal Processing I: Linear Filters*, Springer-Verlag, New York, 1981.

[26] Y. Kamp and J. P. Thiran, "Maximally flat nonrecursive two-dimensional digital filters," *IEEE Trans. Circuits and Systems,* vol. CAS-21, pp. 437-449, May 1974.
[27] Y. Kamp and J. P. Thiran, "Chebyshev approximation for two-dimensional nonrecursive digital filters," *IEEE Trans. Circuits and Systems,* vol. CAS-22, pp. 208-218, 1975.
[28] H. Kato and T. Furukawa, "Two-dimensional type-preserving circular windows," *IEEE Trans. Acoustics, Speech, and Signal Processing,* ASSP-29, pp. 926-928, 1981.
[29] A. H. Kayran and R. A. King, "Design of recursive and nonrecursive fan filters with complex transformations", *IEEE Trans. Circuits and Systems*, vol. CAS-30, pp. 849-857, Dec. 1983.
[30] C.-L. Lau and R. Ansari, "Two dimensional digital filter and implementation based on generalized decimation," *Princeton Conference*, Princeton NJ, March 1986.
[31] C-L. Lau and R. Ansari, "Design of two-dimensional filters using sampling rate alteration", *IEEE Int. Symposium on Circuits and Systems,* pp. 474-477, 1984.
[32] J. S. Lim, *Two-Dimensional Signal and Image Processing*, Prentice-Hall, Englewood Cliffs, NJ, 1990.
[33] Y. C. Lim and Y. Lian, "The optimum design of one- and two-dimensional FIR filters using the frequency response masking technique," *IEEE Trans. Circuits and Systems II: Analog and Digital Signal Proc.,* Vol. 40, pp. 88-95, 1993.
[34] J. H. Lodge and M. M. Fahmy "An efficient l_p optimization technique for the design of two-dimensional linear-phase FIR digital filters," *IEEE Trans. Acoustics, Speech, and Signal Processing,* ASSP-28, pp. 308-313, 1980.
[35] J. H. McClellan, "The design of two-dimensional filters by transformations," *Proc. 7th Annual Princeton Conf. Information Sciences and Systems,* pp. 247-251, 1973.
[36] J.H. McClellan and D.S.K. Chan, "A 2-D FIR filter structure derived from the Chebyshev recursion," *IEEE Trans. Circuits and Systems,* Vol. 24, pp. 372-378, 1977.
[37] W. F. G. Mecklenbrauker and R. M. Mersereau, "McClellan transformation for 2-D digital filter ing: II-implementation," *IEEE Trans. Circuits and Systems,* CAS-23, pp. 414-422, 1976.
[38] R. M. Mersereau, D. B. Harris, and H. S. Hersey, "An efficient algorithm for the design of two-dimensional digital filters", *Proc.* 1974 *Int. Symposium Circuits and Systems* pp. 443-446, 1975.
[39] R. M. Mersereau, W. F. G. Mecklenbrauker, and T.F. Quatieri, Jr., "McClellan transformation for 2-D digital filtering: I-design," *IEEE Trans. Circuits and Systems,* CAS-23, pp. 405-414, 1976.
[40] R. M. Mersereau, "The design of arbitrary 2-D zero-phase FIR filters using transformations," *IEEE Trans. Circuits and Systems,* pp. 372-378, vol. 27, 1980.
[41] R. M. Mersereau and T. C. Speake, "The processing of periodically sampled multidimensional signals," *IEEE Trans. Acoustics, Speech, and Signal Processing,* vol. ASSP-31, pp. 188-194, Feb. 1983.
[42] D. T. Nguyen and M. N. S. Swamy, "Scaling free McClellan transformation for 2-D digital filters", *IEEE Trans. Circuits and Systems,* CAS-33, pp. 108-109, Jan. 1986.
[43] T. W. Parks and J.H. McClellan, "Chebyshev approximation for nonrecursive digital filters with linear phase," *IEEE Trans. Circuits Theory,* Vol. 19, pp. 189-194, 1972.
[44] S. -C. Pei and J. -J. Shyu, "Design of 2-D FIR digital filters by McClellan transformation and least squares eigencontour mapping," *IEEE Trans. Circuits and Systems II: Analog and Digital Signal Proc.,* Vol. 40, pp. 546-555, 1993.
[45] E. Z. Psarakis and G. V. Moustakides, "Design of two-dimensional zero-phase fir filters via the generalized McClellan transform," *IEEE Trans. Circuits and Systems,* pp. 1355-1363, vol. CAS-38, Nov. 1991.
[46] P.K. Rajan, H.C. Reddy, and M. N. S. Swamy, "Fourfold rational symmetry in two-dimensional FIR digital filters employing transformations with variable parameters," *IEEE Trans. Acoustics, Speech, and Signal Processing,* ASSP-31, pp. 488-499, 1982.
[47] V. Rajaravivarma, P. K. Rajan, and H. C. Reddy, "Design of multidimensional FIR digital filters using the symmetrical decomposition technique", *IEEE Trans. Signal Processing,* vol. 42, pp. 164-174, Jan. 1994.
[48] T. Speake and R. M. Mersereau, "A comparison of different window formulas for two-dimensional FIR filter design," *Proc. IEEE Int. Conf. Acoustics, Speech, and Signal Processing,* pp. 5-8, 1979.

[49] S. Treitel and J. L. Shanks, "The design of multistage separable planar filters," *IEEE Trans. Geoscience Electronics,* GE-9 pp. 10-27, 1971.
[50] G. J. Tonge, "The sampling of television images", Independent Broadcasting Authority, Experimental and Development Report 112/81.
[51] M. Vetterli, "A theory of multirate filter banks," *Signal Processing,* vol. 6, February 1984, pp. 97-112.
[52] E. Viscito and J. P. Allebach, "The analysis and design of multidimensional FIR perfect reconstruction filter banks for arbitrary sampling lattices", *IEEE Trans. on Circuits and Systems,* vol. CAS-38, pp. 29-41, Jan. 1991.
[53] J. W. Woods and S.D. O'Neill, "Subband coding of images," *IEEE Trans. Acoustics, Speech, and Signal Processing,* ASSP-34, pp. 1278-1288, 1986.
[54] J. W. Woods, Ed., *Subband Image Coding,* Kluwer Academic Publishers, Norwell, MA, 1990.
[55] T.-H. Yu and S. K. Mitra, "A new two-dimensional window," *IEEE Trans. Acoustics, Speech, and Signal Processing,* ASSP-33, pp. 1058-1061, 1985.

Further Information

Most of the research articles describing the advances in 2-D FIR filter design methods appear in *IEEE Transactions on Signal Processing, IEEE Transactions on Image Processing, IEEE Transactions on Circuits and Systems*, and *Electronics Letters*, and *International Conference on Acoustics, Speech, and Signal Processing* (*ICASSP*) and *International Symposium on Circuits and Systems*.